



THE UNIVERSITY *of* EDINBURGH

Edinburgh Research Explorer

Electrospun Nanofibers for Drug Delivery and Biosensing

Citation for published version:

Cleeton, C, Keirouz, A, Chen, X & Radacsi, N 2019, 'Electrospun Nanofibers for Drug Delivery and Biosensing', *ASC Biomaterials Science & Engineering*, vol. 2019, no. 5, pp. 4183-4205.
<https://doi.org/10.1021/acsbomaterials.9b00853>

Digital Object Identifier (DOI):

[10.1021/acsbomaterials.9b00853](https://doi.org/10.1021/acsbomaterials.9b00853)

Link:

[Link to publication record in Edinburgh Research Explorer](#)

Document Version:

Peer reviewed version

Published In:

ASC Biomaterials Science & Engineering

General rights

Copyright for the publications made accessible via the Edinburgh Research Explorer is retained by the author(s) and / or other copyright owners and it is a condition of accessing these publications that users recognise and abide by the legal requirements associated with these rights.

Take down policy

The University of Edinburgh has made every reasonable effort to ensure that Edinburgh Research Explorer content complies with UK legislation. If you believe that the public display of this file breaches copyright please contact openaccess@ed.ac.uk providing details, and we will remove access to the work immediately and investigate your claim.



Electrospun Nanofibers for Drug Delivery and Biosensing

Conor Cleeton, Antonios Keirouz, Xianfeng Chen, and Norbert Radacsi

ACS Biomater. Sci. Eng., **Just Accepted Manuscript** • DOI: 10.1021/
acsbiomaterials.9b00853 • Publication Date (Web): 12 Aug 2019

Downloaded from pubs.acs.org on August 16, 2019

Just Accepted

“Just Accepted” manuscripts have been peer-reviewed and accepted for publication. They are posted online prior to technical editing, formatting for publication and author proofing. The American Chemical Society provides “Just Accepted” as a service to the research community to expedite the dissemination of scientific material as soon as possible after acceptance. “Just Accepted” manuscripts appear in full in PDF format accompanied by an HTML abstract. “Just Accepted” manuscripts have been fully peer reviewed, but should not be considered the official version of record. They are citable by the Digital Object Identifier (DOI®). “Just Accepted” is an optional service offered to authors. Therefore, the “Just Accepted” Web site may not include all articles that will be published in the journal. After a manuscript is technically edited and formatted, it will be removed from the “Just Accepted” Web site and published as an ASAP article. Note that technical editing may introduce minor changes to the manuscript text and/or graphics which could affect content, and all legal disclaimers and ethical guidelines that apply to the journal pertain. ACS cannot be held responsible for errors or consequences arising from the use of information contained in these “Just Accepted” manuscripts.

Electrospun Nanofibers for Drug Delivery and Biosensing

Conor Cleeton¹, Antonios Keirouz¹, Xianfeng Chen², Norbert Radacsi^{1*}

¹The School of Engineering, Institute for Materials and Processes, The University of Edinburgh, Robert Stevenson Road, Edinburgh, EH9 3FB, United Kingdom

²School of Engineering, Institute for Bioengineering, The University of Edinburgh, King's Buildings, Mayfield Road, Edinburgh EH9 3JL, United Kingdom

*Corresponding author. Tel.: +44 (0) 131 651 7112. E-mail address: n.radacsi@ed.ac.uk

ABSTRACT: Early diagnosis and efficient treatment are of paramount importance to fight cancers. Monitoring the foreign body response of a patient to treatment therapies also plays an important role in improving the care that cancer patients receive by their medical practitioners. As such, there is extensive research being conducted into ultrasensitive point-of-care detection systems and “smart” personalized anti-cancer drug delivery systems. Electrospun nanofibers have emerged as promising materials for the construction of nanoscale biosensors and therapeutic platforms due to their large surface areas, controllable surface conformation, good surface modification, complex pore structure, and high biocompatibility. Electrospun nanofibers are produced by electrospinning, which is a very powerful and economically viable method of synthesizing versatile and scalable assemblies from a wide array of raw materials. This review describes the theory of electrospinning, achievements, and problems currently faced in producing effective biosensors/drug delivery systems, in particular, for cancer diagnosis and treatment. Finally, insights into future prospects are discussed.

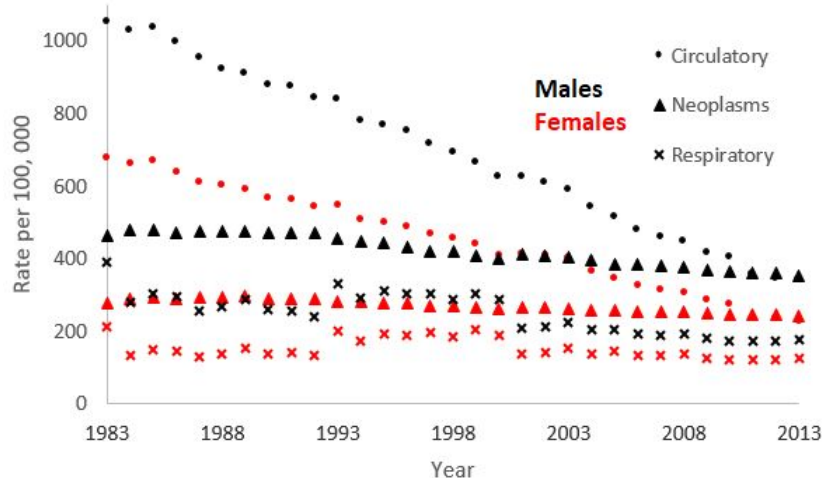
KEYWORDS: Electrospinning, nanofibers, drug delivery, biosensing, cancer

1. INTRODUCTION

Mortality statistics by geographical location reflects a concerning consistency in cancer. It accounts for a large proportion of recorded deaths in many areas of the world, with 9 million deaths by cancer being approximated worldwide in 2016,¹ accounting for 15.8% of the overall 57 million reported deaths. Some technological advancements in the past decades have provided the necessary framework to address some of the medical issues associated with specialized therapy procedures. In almost all cancers, the average 5-year survival rate has improved by up to 2.3% in 2016 alone.² Nevertheless, mortality rates for neoplastic related deaths have declined in a comparatively stagnant fashion relative to circulatory diseases over the past three decades (**Figure 1**). Currently, employed methods of treatment include a combination of surgery, chemotherapy, radiation therapy, immunotherapy, and target-specific therapies.³ A fundamental shortcoming of these treatments is that they are often implemented as part of a mitigating methodology when cancer diagnostics have identified malignant tumors.

The need to pursue more effective means of cancer treatment becomes clear when currently employed methods are considered. Synergistic radiotherapy / surgical resection and systemic chemotherapy – the commonly applied therapeutic strategy⁴ – are limited in their application due to adverse health effects that accompany their administration. In the absence of selectivity for neoplastic cells, common health side effects that are observed might include kidney malfunction, nerve injury, nausea and vomiting,⁵ normal cell toxicity, and death due to extreme dosages.⁶ This is a direct result of the traditional drug delivery process, i.e., *repeated* administration of treatment via the oral or parenteral route⁷. Naturally, with each dosage cycle, the drug concentration in the blood quickly rises and then declines.⁶ As every drug has a plasma concentration above which it is toxic and below which it is useless,⁸ this method of administration is susceptible to accidental or intentional overdose, substance abuse, or simple ineffectiveness.⁷ As such, nanoscale therapeutics have currently been the focus of much

1
2
3 experimental effort due to their ‘biomimetic’ approximation of the extracellular matrix
4 (ECM)’s topography, allowing specific unloading of therapeutic cargo at the tumor site without
5
6
7
8 systemic administration.^{6,7} At the expense of lower loading capacity, the nanometer scale
9
10 allows drug-delivery across the cell membrane, which simultaneously minimizes drug uptake
11
12 by the reticuloendothelial system and unwanted clearance from the body through the spleen or
13
14 liver,⁹ the net effect of which is an improved therapeutic index relative to traditional drug
15
16
17 delivery.



36 **Figure 1.** Age-standardized mortality rates by cause of death from 1982-2013. Produced by the
37 authors using published U.K. government statistics.²

41
42 In recent years, the ability to design novel approaches for cancer treatment has been
43 facilitated by a greater understanding of the tumor microenvironment.¹⁰ For example, as
44 neoplastic cells overexpress certain proteins and characteristic biomarkers, we could design
45 platforms to target them. The advent of nanoscale technology has provided great opportunities
46 in therapeutic treatment, with the potential to create “smart”, personalized anti-cancer
47 therapies, and a new generation of biosensors¹¹ designed to detect a specific biological
48 analyte.¹² For instance, nanomaterials derived from inorganic and carbonaceous materials have
49 been developed for fabricating, e.g. volatile organic compound sensors for cancer diagnostic
50
51
52
53
54
55
56
57
58
59
60

1
2
3 purposes.¹³ However, poor thermal stability and selectivity to the desired biological analyte
4
5 have imposed several practical limitations in employing them for routine clinical application.¹⁴
6
7 Nanoparticles and hydrogels have been identified as potentially valuable platforms for *in vivo*
8
9 cancer therapy as they allow for targeted and/or local delivery of therapeutic agents. However,
10
11 their efficacy is constrained by short circulation times in the case of nanoparticles, and by
12
13 significant wash-out of encapsulated drugs during the gelation period in the case of hydrogels.¹⁵
14
15

16
17 Among the numerous nanomaterials, recently, electrospun nanofibers (ESNFs) have
18
19 attracted much interest as a construction material for drug delivery platforms/biosensors due to
20
21 their large surface area, controllable surface conformation, good surface modification, complex
22
23 pore structure, and high biocompatibility.^{11,16–19} Due to their high drug loading efficiency and
24
25 increased surface-to-volume area, ESNFs are in many ways superior to other small drug
26
27 carriers as they allow for the administration and delivery of substances via a range of different
28
29 routes. ESNFs can be dispensed in the body through common (oral, buccal, sublingual, rectal,
30
31 vaginal, etc.)^{20–22} and topical (transdermal, ocular, inhalation)²³ routes or in the form of local
32
33 or loco-regional implants. ESNFs also allow topical controlled drug release, that makes them
34
35 optimal for cancer therapy.¹⁵ Furthermore, electrospun nanofibers can be biodegradable, unlike
36
37 silicone-based ones. Electrospun nanofibers have better *in vitro* and *in vivo* sensitivity than
38
39 other sensors due to their small size and the enhancement of the mass transport limiting
40
41 membrane.²⁴ Furthermore, biomimetic coatings that can be achieved by electrospinning, which
42
43 can prevent biofouling, thus increase the lifetime of biosensors.²⁴ ESNFs are produced by the
44
45 process of electrospinning, which permits a simple, variable, and effective synthetic route to
46
47 prepare and control the production of nanofibers. Moreover, ESNFs have been fabricated and
48
49 hybridized with functional additives to diversify their application to many fields. This review
50
51 seeks to investigate the novel approaches in designing biosensors based on electrospun
52
53 nano/microfibers and study their applications from the development of ultrasensitive sensors
54
55
56
57
58
59
60

1
2
3 to drug delivery systems. Additionally, the pharmacokinetics of antineoplastic agents
4 incorporated with nanofibers in mediating tumor area-specific release will be examined.
5
6 Contributions from various research groups in this field will give a clear indication of the
7
8 origins, current status, and potential development of ESNF-based biosensors for use in cancer
9
10 diagnostics.
11
12
13
14
15
16
17

18 **2. FABRICATION OF NANOFIBERS BY ELECTROSPINNING**

19 **2.1 Electrospinning process**

20
21
22
23 Electrospinning is a highly versatile method to process solutions, suspensions or melts,
24 into continuous fibers with nano/microscale diameters.²⁵ It is the only method for mass-
25 producing continuous long nanofibers.²⁶ The process uses a high voltage that charges the liquid
26 inside a metallic capillary. A standard laboratory-scale setup consists of four main components:
27 a high voltage power supply, a syringe pump, a nozzle (usually metallic), and a collector (which
28 can simply be metallic foil/plate/disk).²⁷ The electrostatic force produced by the high voltage
29 supply is applied to a polymer solution or melt, which is dispensed through the fine needle
30 orifice at a controlled rate. Accumulated charge at the spinneret orifice subjects the discharged
31 polymer melt to an electric field, which induces a conically-shaped geometry to form (termed
32 the ‘Taylor cone,’ **Figure 2.B**).^{11,27} Increasing the strength of the electric field increases the
33 accumulated charge on the surface of the budding polymer droplet, generating repulsive
34 electric forces that overcome the surface tension of the polymer solution/melt.¹⁸ The resulting
35 jet that is dispensed from the tip of the Taylor cone experiences electrical instabilities by the
36 applied electric field, which causes it to elongate through the application of a mechanical force
37 (**Figure 2.A**). The drawn polymer thread is directed to the oppositely charged or grounded
38
39
40
41
42
43
44
45
46
47
48
49
50
51
52
53
54
55
56
57
58
59
60

collector, and the residual solvent evaporates leaving only the charged polymer fiber on the collector mat (**Figure 2.C**).¹⁹

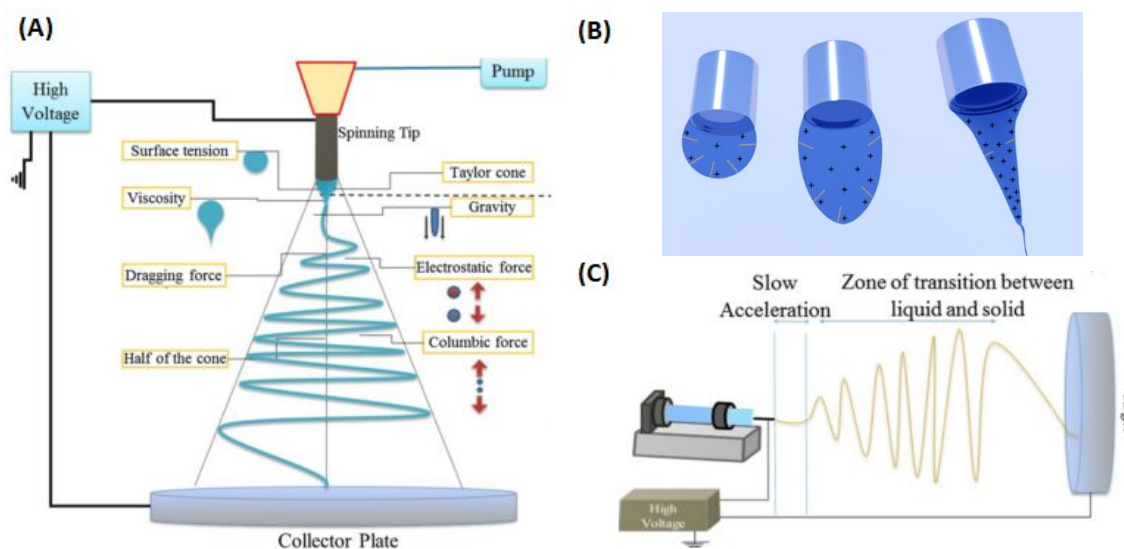


Figure 2. Needle Electrospinning. **(A)** Schematic diagram of an electrospinning needle system using a single needle in a vertical configuration.²⁸ **(B)** Forces acting on the tip of spinneret during the formation of a Taylor cone. **(C)** Horizontal configuration needle electrospinning.²⁸ Setups represented with a static collector plate, but other configurations exist. Panels A and C reproduced with permission from ref 28. Copyright 2017 Elsevier.

Panel B adapted with permission from ref 29. Copyright 2009 IIT Delhi.

2.2 Electrospinning parameters and their influence on fiber morphology

The collected fibers have a nano/microscale diameter with improved modular strength.^{11,27} They also resemble the ECM, making them ideal candidates for biological use. In order to use the produced electrospun fibers for biosensing, their morphological properties often need to be tweaked to produce patterned nanostructures with the objective of optimizing performance parameters of bioreceptors (e.g., response time, stability, and sensitivity).^{11,27} This is often achieved by using additives during or after the electrospinning process, which are immobilized inside or on the surface of the nanofibers.³⁰ The recognition element is interfaced to an

1
2
3 immobilized bioreceptor and signal transducer (e.g., an electrochemical, optical, mass, or
4 calorimetric- based transducer) which amplifies bioassay signal outputs for data processing.³¹
5
6
7 After detection, novel approaches to introducing additives in the form of chemotherapeutic
8 agents favor local drug delivery systems (DDS), where antineoplastic drugs are encapsulated
9 or loaded on biodegradable nanofiber (NF) scaffolds.¹⁹ The immobilization of the additives
10 (e.g., bioreceptors and/or antineoplastic agents) is dependent on the physical and chemical
11 properties of the NF-interstitial matrix, and the interactions between them.¹¹ Each component
12 of the biosensor contributes heavily to its functionality and effectiveness; as such, careful
13 modification of electrospinning parameters - which generates an array of morphologies -
14 addresses this highly selective behavior. **Table 1** summarizes the parameters that influence
15 fiber morphology.
16
17
18
19
20
21
22
23
24
25
26
27
28
29
30
31
32
33
34
35
36
37
38
39
40
41
42
43
44
45
46
47
48
49
50
51
52
53
54
55
56
57
58
59
60

Table 1. Parameters of electrospinning and their influence on fiber morphologies.^{11,19}

Parameter		Influence
Solution Parameter	Viscosity	Fiber diameter increases and the bead formation decreases with increased viscosity
	Molecular Mass	Influences viscosity (<i>vide supra</i>); higher molecular mass results in a more uniform morphology
	Concentration	Increases viscosity and amount of deposited nanofibers
	Conductivity	Fiber diameter decreases with increasing conductivity; ionic materials can reduce atomization of polymer jet
Solvent Properties	Surface Tension	Bead formation may occur if surface tension is considerable (relative to the viscosity)
	Vapor Pressure	Influences solvent evaporation during spinning; solvent evaporation may influence the formation of non-cylindrical morphologies
Operating Conditions	Applied Voltage	Decreasing fiber diameter with increasing voltage supply
	Solution Flow Rate	Lower flow rates = smaller diameter fibers Higher flow rates = larger diameter fibers and/or non-dry fiber deposition at the collector surface
	Distance of collector from nozzle	Fiber solidification; deposition area, increases with increased distance between collector and nozzle
	Collector Type	Aligned fibers, yarns, braided, or random fibers can be obtained by changing from a plate to a drum, area, etc. type collector
	Tip	Hollow or blended fibers may be obtained; increasing tip diameter increases the final fiber diameter
Surrounding Conditions	Temperature	Influences the fiber diameter through temperature-viscosity relationship indirectly (decrease in viscosity with an increase in temperature), and directly increases the product yield/fiber diameter by changing the evaporation rate of the solvent
	Humidity	High humidity may result in circular pore formation in fibers, which can lower the solvent evaporation rate. Low humidity may produce thicker fibers, due to rapid solvent evaporation. Further, high humidity can affect the total charge distribution on the Taylor cone, reducing the surface charge density and thus affecting the electrospinnability of the polymer solution.

2.3. Properties of electrospun nanofibers with different morphologies

Of interest to biosensor applications (aside from the standard smooth surface, solid interior NF) are the porous,^{32–34} nanoparticle-decorated,^{35,36} core-shell,^{28,37} and hollow^{7,38,39} nanostructures (**Figure 3**).

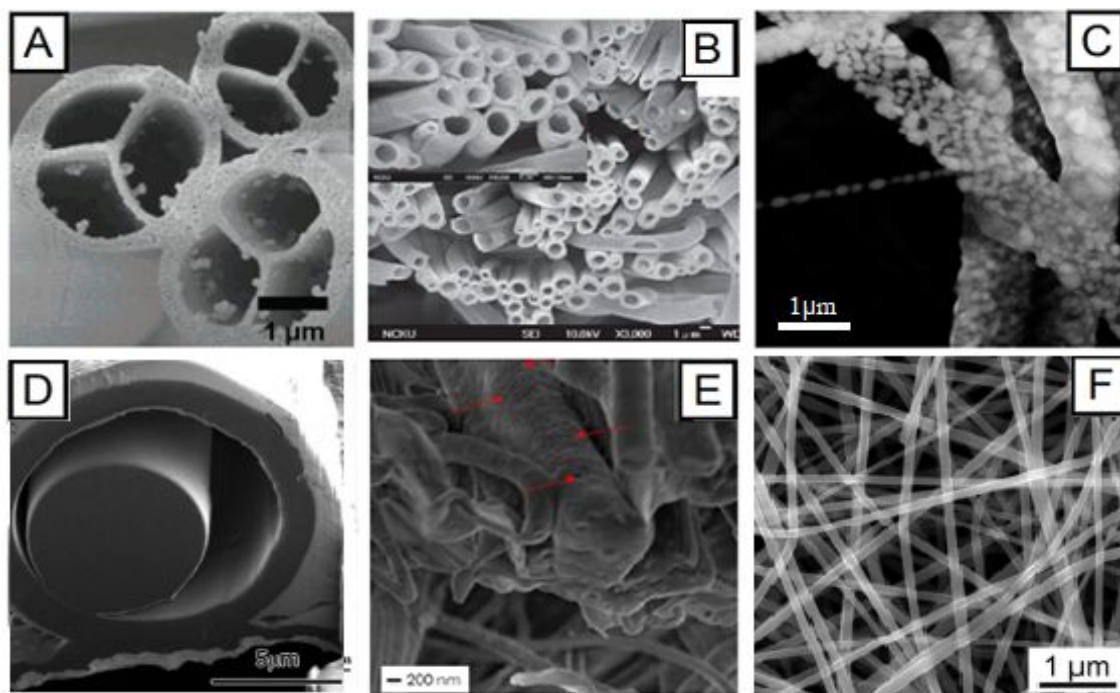


Figure 3. Fiber Morphologies: (A) Biomimetic multichannel microtubes. (B) Hollow nanofibers. (C) Nanoparticle-decorated nanofibers. (D) Core-shell nanofibers. (E) Porous nanofibers (red arrows depict pore structures). (F) Single electrospun nanofibers. Panel A reproduced with permission from ref 40. Copyright 2007 American Chemical Society. Panel B reproduced with permission from ref 41. Copyright 2010 American Chemical Society. Panels C and E reproduced with permission from ref 36. Copyright 2018 Radacsi, N.; Campos, F. D.; Chisholm, C. R. I.; Giapis, K. P. Panel D reproduced with permission from ref 42. Copyright 2012 Elsevier. Panel F reproduced with permission from ref 43. Copyright 2019 American Chemical Society.

These specially fabricated morphologies have higher surface areas than the solid interior NFs, with a greater number of immobilization sites to interface receptors to and improve the performance of ESNF biosensors; **Table 2** compares the relative merits and shortcomings of each morphology.

Table 2. Comparisons of the advantages and disadvantages of core-shell, porous, and hollow electrospun morphologies.¹⁶

Morphology	Advantages	Disadvantages
Core-Shell	<ul style="list-style-type: none"> - Large surface area - Unique properties - Selectable Core & Shell materials 	<ul style="list-style-type: none"> - Complex synthetic route - Harsh post-treatments (which may denature biological components)
Porous	<ul style="list-style-type: none"> - Simple to synthesize - Versatile application - Equipment-independent 	<ul style="list-style-type: none"> - Complex pretreatment required - Uncontrollable loading of nanoscale building blocks
Hollow	<ul style="list-style-type: none"> - Large surface area 	<ul style="list-style-type: none"> - Specific equipment required - Complex synthetic route

Co-axial electrospinning is performed by fitting a small capillary inside a larger outer capillary. The inner capillary contains the core polymer, while the outer capillary produces the shell polymer.³⁷ The polymer solutions are discharged while being subjected to an applied electrical field, conceptually similar to the single-solution electrospinning technique.²⁷ The interactions that govern the resultant core-shell NF properties are derived from the degree of rheological, physical, and chemical dissimilarity between the two polymer solutions;²⁸ however, a uniformly incorporated core-shell fiber is expected to form if a stable Taylor cone is maintained.⁴⁴ Processing parameters related to coaxial electrospinning are reviewed in numerous literature sources,^{41,45} all of which agree that the complexity of coaxial electrospinning originates from the difficulty in maintaining a stable Taylor cone. To induce a stable Taylor cone, process parameters should be such that: (1) An electrospinnable shell solution is utilized; (2) the shell solution viscosity is higher than the core solution viscosity (so that viscous stresses between the core and shell solutions overcome the interfacial tension between them)⁴⁶; (3) a low vapor pressure solvent is used (fast evaporation may destabilize the

1
2
3 Taylor cone); and (4) a greater shell solution conductivity is used (to inhibit core-shell
4 structural discontinuities induced by rapid core polymer elongation).²⁸
5
6

7
8 Hollow NFs may be produced using the co-axial electrospinning technique. Co-axial
9 production of nanotubes was first introduced by Loscertales et al.⁴⁷ and Li & Xia⁴⁸ in 2004,
10 presenting a single-step synthesis of hollow NFs by coaxially electrospinning two *immiscible*
11 liquids. A shell-forming sol constituent is gelled prior to being electrospun with an inert,
12 immiscible core liquid, after which charge induced mechanical forces break up the nanojet,
13 forming hollow NFs with liquid-filled cores. Evaporation of the liquid-filled core during NF
14 elongation leaves only hollow NFs. Loscertales et al.⁴⁷ postulated that in order to maintain the
15 hollow fiber morphology, the shell material should be able to withstand the capillary forces
16 generated after core removal. Similarly, Li & Xia⁴⁸ stated that the presence of a ceramic sol-
17 gel precursor in the shell material was a necessary requirement in order to form stable coaxial
18 jets with robust tubular structures. In this, the fabrication process for hollow morphologies is
19 more stringent compared to porous morphologies (similar to that of the core-shell
20 morphology); however, the resultant surface area is greater,⁴⁹ corresponding to a greater
21 loading capacity for immobilizing transducing elements.
22
23
24
25
26
27
28
29
30
31
32
33
34
35
36
37
38
39

40 Porous nanostructures can be obtained by blending removable inorganic nanoscale
41 building blocks into polymeric matrices and post-treating with organic solvents, removing the
42 nanoscale building blocks to produce porous NFs.²⁷ Additionally, polymeric porogens may be
43 utilized as sacrificial polymer templates, whereby differences in physical properties between
44 the electrospun NF-polymeric porogen matrix (synthesized using simple electrospinning
45 techniques) is exploited in post-treatment processes to remove the porogen component.¹⁶
46
47
48
49
50
51
52
53

54 Nanoparticle-decorated nanofibers can be prepared in one step (during the electrospinning
55 process) or in multiple steps (deposition of nanoparticles after the electrospinning). The
56 addition of nanoparticles on the surface of electrospun nanofibers can provide secondary or
57
58
59
60

1
2
3 tertiary functions that serve to improve upon the performance of non-functionalized
4
5 nanofibers,^{35,36}
6
7
8
9
10

11 **3. ELECTROSPUN FIBERS IN BIOMEDICAL APPLICATIONS**

12
13
14 The structure produced by the electrospinning setup provides a spatiotemporal
15 configuration with the ability to sequester stimulants in various compartments, similar to *in*
16 *vivo* conditions.²⁸ This means that it is possible to modulate the release kinetics of various
17 antineoplastic agents by manipulating the fiber thickness and localization. The release of
18 cytotoxic treatment is unfortunately limited by the pore architecture of NF matrices through
19 which it is dispersed. An NF mesh with a too small diameter-to-porosity ratio will impede the
20 incorporation of interstitial additives into the scaffold material.²⁸ This characteristic is desirable
21 in barrier applications for the skin and endothelium, but not efficient for cancer treatment and
22 detection.⁵⁰ Integrins (more specifically $\alpha\beta3$, a class of animal transmembrane proteins
23 involved in cell-cell adhesion and substrate engagement) are known to play an important role
24 in cytoskeletal organization of the cellular membrane.⁵¹ Integrin expression is upregulated on
25 angiogenic endothelial cells; if $\alpha\beta3$ is blocked with selective antibodies or (Arginine-Glycine-
26 Aspartic acid)-containing peptides, angiogenic endothelial cells *in vivo* will possibly disrupt
27 metastatic mechanisms and undergo apoptosis.^{52,53} Aside from the chemical signaling initiative
28 provided by the interstitial additive, the topological features of ESNFs predominate in the
29 foreign body response of patients, suggesting mechanisms that potentially hinder or accelerate
30 the migration and binding of target-moieties to biosensors.⁵¹ Therefore, ESNFs assembled to
31 approximate an ECM architecture can, to a degree, control the activity of integrins; otherwise,
32 there may be counteracting integrin-dependent proliferation signals.⁵² Brigger et al.⁵⁴
33 developed this idea in their research into nanoparticle DDSs (of the nanosphere, polymeric
34
35
36
37
38
39
40
41
42
43
44
45
46
47
48
49
50
51
52
53
54
55
56
57
58
59
60

1
2
3 matrix variety). They reiterated the potential DDS capabilities of nanoscale polymer matrices,
4
5 postulating the strategy of *in vivo* treatment using drug-loaded colloidal systems. Non-modified
6
7 nanoparticles were rapidly opsonized by macrophages in the mononuclear phagocytes system
8
9 (MPS) (Liver, lungs, spleen, bone marrow), resulting in higher concentrations of administered
10
11 therapeutic agents in the spleen, liver, and lungs of mice. The propensity for MPS macrophages
12
13 to undergo endocytosis/phagocytosis restricted the use of non-surface-modified nanoparticles
14
15 to MPS-specific tumors. Surface characteristics of the traditional nanoparticle matrix were
16
17 modified with hydrophilic-moiety, and the surface curvature has increased above 100 nm,
18
19 reducing opsonization by MPS macrophages and prolonging the DDS' half-life. This allowed
20
21 selective extravasation of cytotoxic agents through the leaky vasculature surrounding
22
23 neoplastic cells, extending its application to tumor sites outside the MPS system. This stresses
24
25 the importance of spatial architecture on effective DDSs and applies equally to any foreign
26
27 substance that is administered into the body of a patient.
28
29
30
31
32

33 For a similar reason, a considerable challenge in the production of nanoscale biosensing
34
35 devices is maintaining bioreceptor functionality.¹¹ For example, incorporation of antibodies as
36
37 an interstitial additive requires a chemically favorable environment in the NF matrix.
38
39 Antibodies can conjugate randomly to nanofibrous surfaces through carbodiimide-mediated
40
41 conjugation routes, which may reduce the activity of the antibody.^{55,56} A study conducted by
42
43 Liang et al.⁵⁷ in 2005 on *in vitro* non-viral gene delivery with nanofibrous scaffolds examined
44
45 the parameters affecting successful transfection. Polylactide-co-glycolide (PLGA) ESNF
46
47 scaffolds were loaded with DNA particles. Two preparation methods were conducted: (1) DNA
48
49 was condensed in a solvent mixture, followed by encapsulation in a triblock copolymer of
50
51 poly(lactide)-b-poly(ethylene glycol)-b-poly(lactide) to form micelles. The micellar mixture
52
53 was electrospun with PLGA to form a nonwoven nanocomposite and nanofibrous scaffold
54
55 (with a core-shell structure) using coaxial electrospinning techniques. (2) DNA was simply
56
57
58
59
60

1
2
3 incorporated with the PLGA and electrospun thusly. The authors⁵⁷ observed that DNA which
4 was not encapsulated in the copolymer was degraded because of the electrospinning process,
5 displaying no transfection. In comparison, the DNA encapsulated in the copolymer was
6 virtually undisturbed, attributable to the core-shell structure protecting the DNA, allowing
7 transfection to take place. The juxtaposition of the two results highlights the difficulty in
8 maintaining bioactivity of interstitial additives. If biological agents are to be incorporated into
9 electrospun structures, then special consideration of the biological function in which they are
10 to be implemented must be upheld. This is of little consequence to the delivery of non-
11 biological therapeutic agents such as *heparin* (an anticoagulant), which has been successfully
12 incorporated in ESNF mats with uniform distributions in previous studies.^{58,59} A polymer melt
13 was prepared by loading heparin in a 7:3 v/v dichloromethane: methanol solution, which was
14 used to dissolve the polymer.⁵⁸ The collected fibers (produced using a flow rate of 0.5 mL h⁻¹
15 of polymer melt and a 0.8 kV cm⁻¹ applied electric field between the capillary and the collection
16 plate) were sterilized in 70% ethanol baths for 15 minutes followed by 5-minute cycle washes
17 in cell culture media. Sustained diffusional release of biologically functional heparin was
18 obtained over a 14-day period, highlighting its validity as a DDS for local administration to the
19 site of vascular grafts. Evidently, the end objective of the electrospinning process demands
20 careful consideration of the factors affecting it, be it biosensing, drug delivery, or otherwise.
21
22
23
24
25
26
27
28
29
30
31
32
33
34
35
36
37
38
39
40
41
42
43
44
45

46 **4. ELECTROSPUN NANOFIBERS FOR BIOSENSORS**

47 **4.1. The Bioreceptor**

48
49
50
51
52 The bioreceptor plays the role of molecular recognition, producing a physiochemical
53 response to interactions with a biological analyte (i.e., biocatalysis, immunological coupling,
54 chemoreception, etc.)³¹ to be detected by a signal-transducing element. The compact analytical
55 device is represented generally in **Figure 4**. It has been noted in many studies that the functional
56
57
58
59
60

significance of biomarkers for early cancer detection is insurmountable. It is not the objective of this literature review to provide an account of biomarkers that have been identified as cancer-indicating. Instead, a partial list of the most promising analytes and their conjugate bioreceptors are provided in **Table 3** to aid the reader in the subsequent discussion.

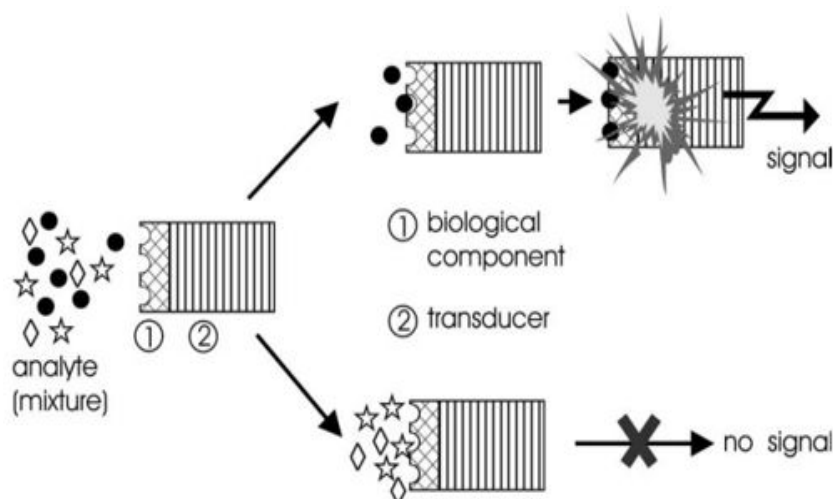


Figure 4. Principle of function of a biosensor. A biological analyte in a complex media specifically interacts with an immobilized bioconjugate on the biosensor surface. The output signal is converted into a physical readout signal via a transducer. Incompatible analytes will not interact to produce a signal output. Reproduced with permission from ref 60. Copyright 2002 Springer-Verlag.

It is interesting to note that despite the exceptionally greater scholarly effort into NF systems for cancer therapeutics (compared to *in vitro* diagnostics), comparatively few have been approved for clinical trial. A study conducted in 2006 reported over 150 companies developing nanoscale therapeutics, with only 23 being approved for clinical use, 3 for *in vivo* imaging, and 2 for *in vitro* diagnostics; collectively the market value was estimated at \$6.2 billion (£14.86 billion, adjusting for inflation).⁶¹ In 2008, the US Federal Drug Administration and European Medicines Agency approved only a few for cancer treatment.⁵⁵ As of 2016, 51 FDA-approved nanomedicines were identified, and a further 77 products were in clinical trial

1
2
3 stages.⁶² The FDA-approved nanotherapeutics were predominantly polymeric, liposomal, or
4
5 nanocrystal formulations; more complex materials comprising micelles or protein-based
6
7 nanoparticles are yet to be FDA-approved. While ESNFs for cancer treatment are mostly in
8
9 their infantile or preclinical stages, it is worth observing that the detection and treatment of
10
11 cancer are synergistic, so for optimal results both the local detection and delivery of cytotoxic
12
13 treatment should be employed clinically. Biosensors are utilized more liberally due to their
14
15 diverse portfolio, including glucose monitoring for diabetes,⁶³ food quality and safety,⁶⁴
16
17 fermentation processes,⁶⁵ and environmental pollution control.⁶⁶ Exploiting biosensors for
18
19 disease screening and diagnostics is not a new concept; however, its employment in
20
21 conjunction with DDSs appears novel. Not including the technological difficulties in
22
23 constructing DDSs and ultrasensitive biosensors, it is evident that legal, ethical, and economic
24
25 restrictions constrain its widespread adoption as primary point-of-care treatment presently.
26
27
28
29
30
31
32

33 **Table 3.** Promising analytes and their conjugate bioreceptors for cancer diagnostics and
34 treatment.

Recognition Element	Analyte	Bioreceptor	Anatomical Relevance in Cancer Detection	Source
Antigen/Antibody	PSA	anti-PSA	Prostate	56,67
	CA 125	anti-CA 125	Ovarian, Uterus, Pancreas, Liver, Colon	12
	CEA	anti-CEA	Breast, Colon	12 28
Enzyme	Glucose	GOx	n/a	63,68
	ITIH4	Peptide-specific antibody	Ovarian, Breast, Colon, Prostate	69
	HRP	H ₂ O ₂	Breast	11
Receptor	HER-2 / EGFR family	anti-HER-2	Breast, Colon, Lungs	55,70
	Folate	Folic acid-liposomal conjugates	Ovarian, Lung, Brain, Head & Neck, Renal	55

Nucleic Acids	p53	n/a	Lung, Neck, Brain, Leukemia, Colon, Breast	71,72,11
---------------	-----	-----	---	----------

PSA = Prostate Specific Antigen; CA 125 = Cancer Antigen 125; CEA = Carcinoembryonic antigen; ITIH4 = Inter-alpha-Trypsin Inhibitor Heavy chain family member 4; HRP = Horse Radish Peroxidase; HER-2 = Human Epidermal growth factor Receptor 2.

4.2. Bioreceptor Immobilization

Part of the construction of biosensors requires immobilization of the bioreceptor onto ESNF matrices by conjugation; this process is selective. This means that an immobilization method optimized for a particular bioreceptor does not apply uniformly to all bioreceptors. Just as conjugation of biological analytes to bioreceptors is selective (**Table 3**), the technique must be adjusted to conform to the unique properties of a given bioreceptor. The typical conjugation routes for tumor targeting is provided in **Table 4**.

Recent advances in bioconjugation techniques have been widely reviewed in the literature;^{73–75} however, a brief outline of the most common techniques prevalent to cancer optimized biosensors will be provided. Immobilization is classified under *reversible* processes (Adsorption and Bioaffinity) and *irreversible* processes (Covalent Binding, Cross-Linking, and Entrapment),⁷⁴ represented in **Figure 5**. Adsorption (physical), bioaffinity, and entrapment are physical methods of immobilization while covalent bonding, adsorption (ionic), and cross-linking are chemical methods.

Table 4. Bioconjugate Components and designs for tumor targeting application.⁷⁵

Bioconjugate Components	Bioconjugate Reagents	Bioconjugate Designs
-------------------------	-----------------------	----------------------

Polymers; dendrimers; cytotoxic agents; toxins; enzymes; prodrugs; haptens or ligands; antibody or antibody fragments	Heterobifunctional aliphatic crosslinkers; heterobifunctional PEG-based crosslinkers; PEGylation agents; multifunctional scaffolds; zero-length crosslinkers; homobifunctional crosslinkers; thiolation reagents; spacer arms	Antibody-drug; antibody-enzyme; antibody-polymer-drugs; antibody-polymer-dye-drug; hapten-drug; ligand-drug
---	---	---

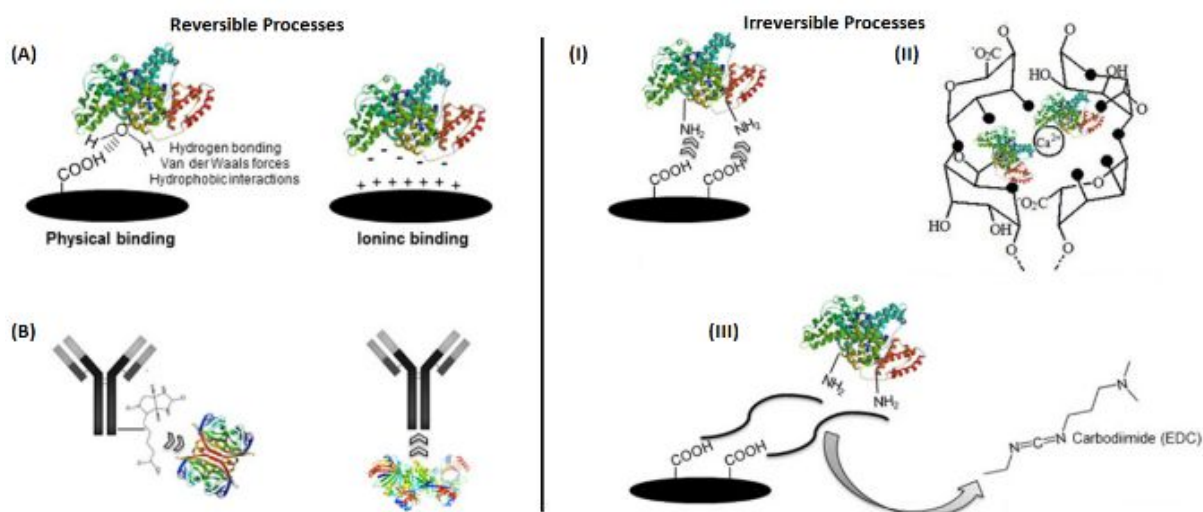


Figure 5. Bioreceptor Immobilization Methods. **(A)** Adsorption, physical and ionic binding. **(B)** Bioaffinity-based immobilization. **(I)** Covalent binding through primary amines. **(II)** Entrapment on beads or fibers and micro-encapsulation. **(III)** Cross-linking using carbodiimide mediated conjugation. Reproduced with permission from ref 73. Copyright

2016 Susana Liébana, Guido A. Drago.

4.2.1. Reversible Processes

Adsorption (by physical or ionic binding) represents the easiest method of immobilization, where the ESNF matrix is enriched with bioreceptor molecules at the vicinity of the interface. Physical adsorption (**Figure 5 (A)**) of the bioreceptor molecules occurs by weak intermolecular interactions (i.e., hydrogen bonding, van der Waals forces or hydrophobic interactions)

1
2
3 between the adsorbate (the bioreceptor) and the adsorbent (the ESNF surface). Ionic
4 chemisorption simply binds the biological agent through salt linkages.
5
6

7
8 Bioaffinity immobilization (**Figure 5 (B)**) occurs via two alternative routes. In the first,
9 the bioreceptor species is conjugated to a ‘fusion tag’ molecule which has an affinity for the
10 ESNF matrix. In the second, the ESNF matrix is activated and precoupled with an affinity
11 ligand, after which the bioreceptor is added. The precoupling process can be conducted by any
12 covalent bonding mechanism used for generating affinity media; however, if the affinity ligand
13 is a biologically active protein, then the precoupling process should optimize the number of
14 accessible binding sites between the target analyte and bioreceptor, which ultimately
15 determines the sensitivity and stability of the biosensor. Even so, the unique characteristics of
16 this method pose some challenges to its eventual commercialization due to affinity ligands
17 being, on occasion, economically infeasible, unstable *in vivo*, or difficult to isolate.⁷⁶
18
19
20
21
22
23
24
25
26
27
28
29
30
31
32

33 **4.2.2. Irreversible Processes**

34
35 Covalent binding (**Figure 5 (I)**) immobilizes the bioreceptor onto the ESNF matrix by
36 covalent bonding. This process is widely used when designing biosensors due to the stability
37 of the bond, which precludes the leaching of bioreceptor molecules into the surrounding
38 solution, thereby allowing prolonged *in vivo* measurements to be taken.⁷⁷ Active binding sites,
39 such as the antibody recognition areas should not be blocked by this process, as this counteracts
40 the objective of biosensing. Generally, five functional groups have been identified as the
41 necessary precursors to covalent binding immobilization in practical conjugation methods.
42 These are: Primary amines ($-NH_2$) (can be targeted without denaturing the bioreceptor using
43 N-hydroxysuccinimidyl ester reactive groups); Carboxy groups ($-COOH$) (usually available on
44 the bioreceptor surface as a C-terminus in polypeptide chains); Thiols ($-SH$) (disulfide bonds
45 between cysteine groups in the bioreceptor can be reduced to thiols using maleimide -or
46
47
48
49
50
51
52
53
54
55
56
57
58
59
60

1
2
3 iodoacetyl-activated reagents for thiol-directed conjugation); Carbonyls (-CHO) (can be
4 created by glycosylation of glycoproteins with sodium meta-periodate); Carbohydrates
5 (oxidized sugars can be reacted to hydrazide-activated groups or primary amines through
6 reductive amination).⁷³
7
8
9
10

11
12 Entrapment is the method of choice for the immobilization of enzymes with low molecular
13 weight substrates in polymeric networks. The occlusion of bioreceptors in the ESNF matrix
14 occurs by physically caging the enzyme (not binding it, see **Figure 5(II)**), allowing substrates
15 and products to selectively permeate through the caged structure while still maintaining
16 bioactivity.⁷⁸ Access to binding sites on the enzyme can be inhibited by the ESNF enclosure,
17 preventing the use of bioreceptors with high molecular weight substrates.
18
19
20
21
22
23
24
25

26 Cross-linking immobilization chemically joins the bioreceptor to the ESNF matrix by an
27 intermediary cross-linker molecule which contains two (or more) reactive functional groups
28 (**Figure 5(III)**). Many cross-linker molecule variants are available for immobilizing specific
29 bioreceptors (**Table 4**). For instance, bioconjugates made with HRP for developing western
30 blots can be immobilized using zero-length cross-linkers, where the carbohydrate on the
31 glycoprotein is oxidized and subsequently coupled to a target molecule by reductive
32 amination.⁷⁵
33
34
35
36
37
38
39
40
41
42
43
44

45 **4.3. The Biosensor**

46
47 The immobilization and stabilization of the bioreceptor occur principally on the
48 transducing element of the ESNF biosensor complex. Occasionally, immobilization may take
49 place on functional additives that are incorporated to improve the analytical performance of the
50 biosensor.⁷³ Transducing elements are categorized into electrochemical, calorimetric-based,
51 optical, or mass-based.¹² Currently, the distribution of reported biosensors favors the use of
52 electrochemical biosensors, with 89% being documented as electrochemical, 9% as optical,
53
54
55
56
57
58
59
60

1
2
3 and 2% as mass or calorimetric.⁵⁶ An earlier analysis in this literature review on the biological
4
5 detection behavior of biosensors has emphasized the importance of bioreceptor functionality.
6
7 In truth, effective transduction of analyte response signals is heavily dependent on the
8
9 dispersion behavior *and* biological compatibility of functional additives in ESNFs; likewise,
10
11 physical characteristics of the transducing elements contribute significantly to the overall
12
13 performance of the biosensor.¹⁶ The following discussion will focus mainly on providing an
14
15 account of ESNF electrochemical biosensors, their synthetic routes, and their application in
16
17 cancer detection. A brief discussion will follow on the use of optical, mass, and calorimetric
18
19 biosensors, and their application in cancer detection.
20
21
22
23
24
25
26

27 **4.3.1. Electrochemical Biosensors**

28
29 Electrochemical biosensors (ECBSs) are currently the most mature biosensing devices
30
31 used in practice.¹² Characteristics of this variant of biosensor, derived from microelectronic
32
33 circuits, include robustness, easy scalability, portability, excellent detection limits (even with
34
35 a small analyte volume), and the ability to be employed domestically as point-of-care devices.¹²
36
37 Principally, the ECBS operates by extracting electrical response signals from biological
38
39 analytes that react electrochemically with the surface of a working electrode. The response
40
41 signal is either a measurable current (*amperometric*; linear concentration dependence), a
42
43 measurable potential (*potentiometric*; logarithmic concentration dependence), or a measurable
44
45 alteration in the conductive properties of a medium between two electrodes (*conductometric*).⁷⁹
46
47 The recognition element is typically an enzyme due to its high catalytic activity and selective
48
49 binding between the analyte and bioreceptor.⁸⁰ However, immunosensors - in which antibodies
50
51 are coupled to electrochemical transducers - have also been widely employed in the
52
53 measurement of cancer biomarkers, especially prostate-specific antigens.⁸¹
54
55
56
57
58
59
60

1
2
3 Electrodes in the ESNF matrix serve as the transducing element of the biosensor, usually
4 requiring a minimum of three to be used in electro-active responses. A *reference electrode*,
5 commonly made of silver, is isolated from the surface reaction and maintained at a fixed
6 potential from which measurements can be compared. The *working electrode (cathodic or*
7 *anodic mode)* transduces the measured electrochemical response, while the *auxiliary electrode*
8 connects the working electrode to an electrolyte solution, inducing a current for operation.⁸²
9
10 The properties of the electrode material influence the response time, stability, and sensitivity
11 of the biosensor, but transducer-immobilized enzymes often exhibit inefficient electron transfer
12 for signal transduction.⁸³ This is the result of unfavorable enzyme orientation to the electrode
13 surface, which inhibits a rapid exchange of electrons. The sensitivities of unaltered ECBSs are
14 rarely useful for biomarker detection as a result. By modifying the transducer with highly
15 conductive and chemically stable additives such as carbon nanotubes (CNTs), metal
16 nanoparticles, and quantum dots (QDs),⁸⁴ it is possible to improve an ECBS's sensitivity and
17 signal-to-noise ratio⁷⁹ through facilitated electron transport between the bioreceptor and
18 electrode.⁷⁷ Furthermore, studies have demonstrated a strong adsorption capacity for enzymes
19 on these nanoscale building blocks, subsequently improving the response time, sensitivity, and
20 stability (by minimizing enzyme unfolding) of ECBSs.⁸⁵ The homogeneous distribution of
21 these nanoscale building blocks is vital to ensure good performance, so dispersion strategies
22 for nanoscale building blocks in ESNF-ECBSs will be discussed.

4.3.1.1. Pre-Processing Modification of Nanoscale Building Blocks in Electrospun

Nanofibers

54 The pre-processing method of ESNFs introduces nanoscale building blocks by adding the
55 desired modifier to the polymer melt before being electrospun into nanofibrous scaffolds.⁸⁶
56 Theoretically, the greater the nanoscale building block content in the polymer melt, the more
57
58
59
60

1
2
3 even the distribution through the ESNF matrix, and the greater the performance of the ECBS.
4
5 These properties are mutually inhibited, however, as nanoscale building blocks have higher
6
7 surface energy than the ESNF matrix often leading to aggregation.¹⁶ Pre-processing methods
8
9 of overcoming this aggregatory behavior include *blending* of nanoscale building blocks
10
11 (through external force-assisted dispersion or anisotropic additive-promoted dispersion) or *in*
12
13 *situ synthesis* of nanoscale building blocks in ESNFs.
14
15
16
17
18
19

20 **4.3.1.1.1. Blending of Nanoscale Building Blocks in Electrospun Nanofibers**

21
22 Dispersion of nanoscale building blocks in ESNFs can be assisted by external driving
23
24 forces - such as ultrasonic treatment or adding surface-active agents¹⁶ - or adding anisotropic
25
26 materials to ESNF matrices, which promotes a more uniform distribution in the polymer melt
27
28 after being electrospun.³⁶ Generally, it is a metal nanoparticles that are loaded in the polymer
29
30 melt for ECBSs due to their good dispersion, and optimal conductive properties,⁸⁶ however,
31
32 organic nanostructures may also be utilized in, for example, near-infrared imaging for early
33
34 cancer detection⁸⁷ or as fluorescence probes for bioimaging.⁸⁸⁻⁹⁰ Diamond nanostructures have
35
36 emerged as attractive materials in biomedical applications such as bioimaging, biosensing, and
37
38 drug delivery due to their exceptional mechanical, thermal, optical, and electrical properties.⁹¹
39
40 Additionally, it has been noted in previous studies that Ag, Au, Pt, Cu, and Ni nanoparticles
41
42 have very good electrochemical activity towards H₂O₂, the analyte conjugated to HRP that is
43
44 prevalent in breast cancer monitoring (see **Table 3**). The works of Devadoss et al.⁹² present
45
46 their findings on synthesizing (Au nanoparticle)-composite Nafion NFs (specifically: (Au
47
48 nanoparticle)-Nafion-polyacrylic acid (PAA) NFs) using the simple electrospinning technique
49
50 outlined in *section 2*. N,N'(4-dimethylamino) pyridine (DMAP) and DMAP-protected (Au
51
52 nanoparticle)-incorporated Nafion NFs were directly mixed and electrospun on a stainless steel
53
54 working electrode, after which HRP was immobilized on the electrode surface by physical
55
56
57
58
59
60

1
2
3 adsorption in the presence of poly(acrylic acid) molecules. Electron microscope imagery
4 compared the (Au nanoparticle)-composite with the (Au nanoparticle)-free composite,
5 revealing a high surface area and uniform distribution of Au nanoparticles in the composite
6 NFs. This homogenous inclusion was attributed to the strong electrostatic interactions between
7 the negatively charged sulfonate groups in Nafion and the positively charged DMAP-protected
8 Au nanoparticles. It was demonstrated that the (Au nanoparticle)-composite electrodes, when
9 employed as reservoirs for horseradish peroxidase immobilization, produced reliable and
10 sensitive electrochemical detection of the enzymatic reaction occurring on the surface. The
11 sensitivity was improved by order of magnitude compared to previous ECBSs (with a limit of
12 detection = 38 nM), and the bioreceptor remained biologically stable for over three weeks.

13
14
15
16
17
18
19
20
21
22
23
24
25
26 A recent review on metal-oxide NF-based ECBSs³⁸ provides an account of current
27 advancements in the production of ESNFs doped with metal-oxide precursors. These metal-
28 oxide NFs are produced by blending an inorganic precursor with a polymer solution and
29 electrospinning using co-axial,^{28,37} colloid-,⁹³ solution- (see *section 2*),⁹⁴ and melt-
30 electrospinning⁹⁵ techniques. While melt-electrospinning eliminates the need for harsh organic
31 solvents, the necessary elevated operating temperatures (between 60°C and 90°C)⁵⁰ may
32 preclude its use in biosensor application by potentially denaturing immobilized enzymes.
33 Nevertheless, a metal-oxide derived ESNF mat can be synthesized by evaporating a sacrificial
34 polymer carrier and oxidizing an inorganic precursor, promoting fiber-aligned, uniform
35 nucleation of metal-oxide nanoscale building blocks in a polymer matrix.³⁸ The resultant
36 morphological properties include a high surface area-to-pore ratio and diverse pore
37 architecture, which increases the number of available bioreceptor binding sites and further
38 improves the biosensor sensitivity. Indeed, mesoporous zinc oxide (ZnO) ESNF-ECBSs with
39 high sensitivity, reproducibility, and stability were successfully fabricated and reported by Ali
40 et al.⁹⁶ for the detection of anti-epidermal growth factor receptor 2 (overexpressed in breast
41
42
43
44
45
46
47
48
49
50
51
52
53
54
55
56
57
58
59
60

1
2
3 cancer patients). High sensitivity ($7.76 \text{ k}\Omega \mu\text{M}^{-1}$), low detection limit (1 fM), fast detection
4 time (128 s), and a broad detection range (1 fM - 0.5 μM) was obtained, corresponding to an
5
6 order of magnitude improvement in sensitivity relative to the then-current best in literature,⁹⁷
7
8 and three orders of magnitude improvement relative to the Enzyme-Linked ImmunoSorbent
9
10 Assay standard for breast cancer biomarker detection. Similarly, ZnO ESNFs doped with
11
12 multiwall carbon nanotubes (MWCNTs) have been produced by blending a three-component
13
14 mixture (of ZnO, MWCNTs, and polymer melt) and electrospinning for use in CA 125 analyte
15
16 detection (see **Table 3**).⁹⁸ Highly oriented ZnO nanowires were embedded in the ESNF matrix
17
18 by a one-step calcination process at a temperature that simultaneously avoided MWCNT
19
20 decomposition and created MWCNT-ZnO functional groups for antibody immobilization,
21
22 resulting in an immunosensor with good dispersion of MWCNTs and high electrocatalytic
23
24 activity. A particularly promising development in the field follows the recently published
25
26 works of Tripathy et al.⁹⁹. The authors present their findings on synthesizing an electrospun
27
28 semi-conducting Manganese (III) Oxide (Mn_2O_3) NF ECBS for DNA hybridization detection.
29
30 The Mn_2O_3 NFs were synthesized by blending a polyacrylonitrile / N,N-dimethylformamide
31
32 polymer matrix with a known weight % of Manganese (II) Acetate tetrahydrate and stirring for
33
34 1 hour at 60°C and then 2 hours at 65 °C. The precursor solution was electrospun to form a
35
36 free-standing nonwoven NF membrane; collected NFs were then calcinated at 500 °C to obtain
37
38 homogeneously dispersed Mn_2O_3 NFs. The DNA probe was immobilized by covalently
39
40 binding the amine groups on the nucleotide to activated carboxylic groups on the Mn_2O_3 NF
41
42 matrix, shown in **Figure 6**.
43
44
45
46
47
48
49
50
51
52
53
54
55
56
57
58
59
60

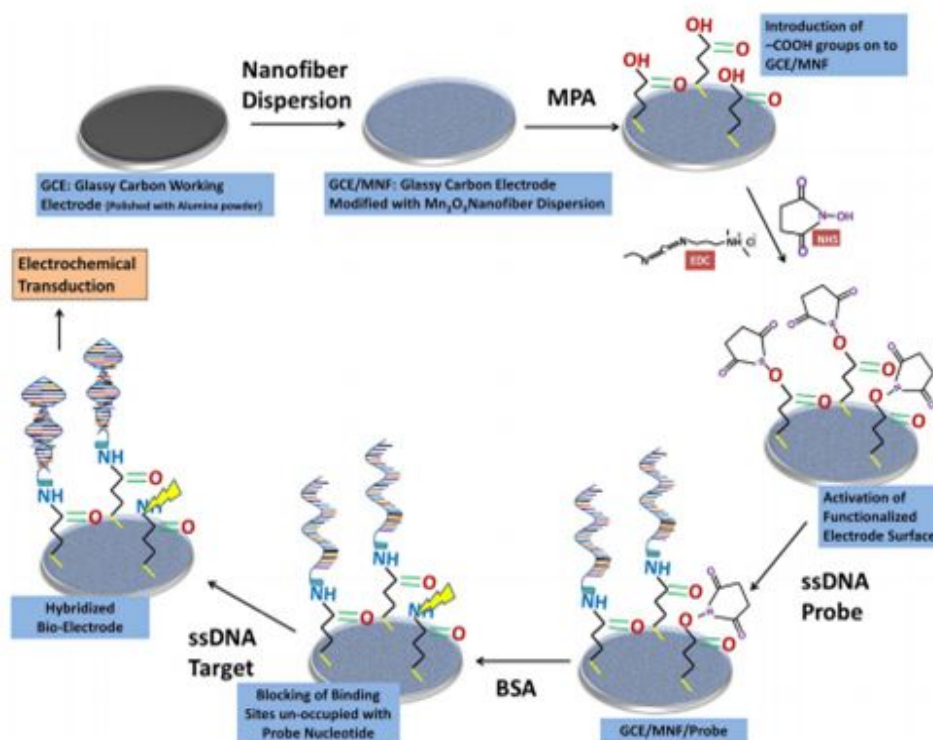


Figure 6. Schematic representation of a proposed DNA-hybridization semi-conducting Manganese (III) Oxide electrochemical biosensor. GCE = Glassy Carbon Electrode, MNF = Modified nanofiber, MPA = Mercaptopropionic acid, EDC = 1-Ethyl-3-(3-dimethylaminopropyl) carbodiimide, NHS = N-hydroxysuccinimide. Reproduced with permission from ref 99. Copyright 2017 Elsevier.

It was demonstrated that the Mn₂O₃-doped ECBS performed better than the unmodified ESNF-ECBS, obtaining unprecedented sensitivities (up to 6.93 kΩ mol⁻¹cm⁻²) and a zeptomolar limit of detection (120 × 10⁻²¹ M). The authors attribute these properties to a decreased charge transfer resistance in the system, promoted by accumulation of negatively charged ssDNA probes on the semiconducting NF coating. Additionally, the accumulated charge produced a Mn₂O₃ NF matrix with a lower band structure than conventionally wide bandgap material approaches, significantly enhancing the limit of detection of biological analytes in ECBSs. This synthetic methodology is especially attractive for biosensors used in cancer detection as the immobilization and functionalization protocols are generic in nature. The ECBS could be extended to any of the recognition elements outlined in **Table 3** simply by modifying the

1
2
3 working electrode with probe sequences specific to the desired biological analyte, providing
4
5 an almost all-inclusive anatomically relevant platform for point-of-care lab-on-chip cancer
6
7 diagnostics.
8
9

10 11 12 13 **4.3.1.1.2. *In Situ* synthesis of Nanoscale Building Blocks in Electrospun Nanofibers**

14
15 *In situ* synthesis requires dispersing metallic ions in a polymer solution before
16
17 electrospinning, thereafter reducing the uniformly distributed ions to metallic nanoscale
18
19 building blocks by heat-, light-, additives, or electro-stimulation.¹⁰⁰ Several medically relevant
20
21 ESNFs have been functionalized with nanoscale building blocks using *in situ* methods,
22
23 including: GNP-doped polyacrylonitrile ECBSs by an oxidation-reduction reaction,¹⁰¹ hybrid
24
25 silica-PVA NFs by sol-gel electrospinning,³² CNT- and Pt nanoparticle-doped polyvinylidene
26
27 difluoride NF membranes for biosensor application,¹⁰² and Ag-doped ZnO nanoparticles on
28
29 electrospun cellulose NF mats by hydrolysis.¹⁰³ As the nanoscale building block precursors are
30
31 added in their ionic form, the aggregatory behavior characteristic of pre-processing blending is
32
33 avoided. In this, *in situ* synthesis is the preferable approach for metal nanoparticles; however,
34
35 this strategy is exclusive to metallic based nanoscale building blocks and cannot be employed
36
37 for doping ESNFs with CNTs, MWCNTs, or other non-metallic nanoscale building blocks.
38
39 Interestingly, there are many instances in literature where metal-oxides have been introduced
40
41 to ESNFs *in situ* as a surface coating.^{33,39,73,104–106} After electrospinning a polymer-precursor
42
43 solution, calcination of the organometallic metal-oxide / sol-gel precursor caused the NF
44
45 diameter to contract. This induced a brittle fiber morphology, onset by internal mechanical and
46
47 thermal stresses.¹⁰⁴ Generally, supplementary materials which are both mechanically and
48
49 chemically stable during the calcination process are embedded in polymer-precursor solutions
50
51 before being electrospun to preserve the ESNF's structural integrity. The principle that only
52
53 surface-bound nanoscale building blocks interact with recognition elements - meaning
54
55
56
57
58
59
60

1
2
3 internally dispersed nanoscale building blocks contribute little to the transduction of biological
4 response signals¹⁰⁷ - suggests that *in situ* surface coated metal-oxide ESNFs are promising
5 materials for biosensor applications. On the nanoscale, however, morphological processing and
6 surface arrangements of nanoscale building blocks are of paramount importance in improving
7 the sensitivity of biosensors to cancerous analytes, an issue which is best addressed by synthetic
8 post-processing routes.
9

20 **4.3.1.2. Post-Processing Modification of Nanoscale Building Blocks in Electrospun**

21 **Nanofibers**

22 The post-processing method of synthesizing ESNFs with nanoscale building blocks
23 requires decorating an as-spun NF matrix with functional additives by various immobilization
24 techniques.
25

33 **4.3.1.2.1. Core-Shell Morphology**

34 Regardless of complex post-treatments restricting its broader application, core-shell NFs
35 have been adopted previously as ESNF-ECBSs for cancer detection. Li et al.¹⁰⁸ reported their
36 findings on synthesizing an immunosensor for CEA-biomarker detection. A nanoporous
37 gold/chitosan modified paper working electrode was used as the sensor platform, and graphene
38 QD functionalized bimetallic Platinum-coated gold (Au@Pt) core-shell nanoparticles were the
39 signal labels.¹⁰⁸ Anti-CEA antibodies were subsequently immobilized by covalent assembly of
40 signal antibodies on graphene QD tagged Au@Pt core-shell nanoparticles, following a
41 sandwich-type immunoreaction in which graphene QDs / Au@Pt labels were captured onto the
42 NGC-PWE surface.¹⁰⁸ The proposed strategy produced an immunosensor with a detection
43 range of 1.0 pg mL⁻¹ - 10 ng mL⁻¹, and a limit of detection of 0.6 pg mL⁻¹, comparable in
44 performance to the best commercial graphene / CNT based ECBSs.¹⁰⁸ The authors also
45
46
47
48
49
50
51
52
53
54
55
56
57
58
59
60

1
2
3 remarked that the synthetic technique they employ can be readily expanded to detecting other
4 cancer biomarkers and that its potential for ultrasensitive cancer diagnostics is very
5 promising.¹⁰⁸
6
7

8
9
10 Core-shell ESNFs have also been fabricated and reported by Li et al.¹⁰⁹ and Shen et al.¹¹⁰
11 as novel H₂O₂ ECBSs. Li et al. constructed a piece of conductive cloth from electrospun
12 polycaprolactone (PCL) NFs decorated with polypyrrole (PPy)-coated silver nanoparticles
13 (Ag@PPy), which formed the core-shell structure of Ag@PPy / PCL@PPy. The flexible
14 conducting cloth was successfully pasted onto a glassy carbon electrode for biosensory
15 application, showing good electrochemical activity toward the direct reduction of H₂O₂ with a
16 limit of detection down to 1 μM and a broad linear detection range of 0.01 mM - 3.5 mM.
17 Likewise, Shen et al. described the synthesis of a novel core-shell hybrid H₂O₂ biosensor,
18 utilizing both *in situ* and synthetic post-processing routes. SiO₂@Au NFs were produced by
19 electrospinning a silica sol precursor, after which gold seed particles were grown *in situ* via a
20 layer-by-layer self-assembly method. Gold shells were then used to encapsulate the SiO₂@Au
21 NFs, forming the gold-coated silica fiber hybrid material. The nanocomposite displayed
22 excellent chemical stability, biocompatibility (with horseradish peroxidase, see **Table 3**), as
23 well as a high sensitivity (from 5 μM to 1 mM with a limit of detection of 2 μM), indicative of
24 an ECBS platform with a high level of variability.
25
26
27
28
29
30
31
32
33
34
35
36
37
38
39
40
41
42
43
44
45
46

47 **4.3.1.2.2. Porous Morphology**

48
49 Cui et al.¹¹¹ constructed a carbon NF-hydroxyapatite (HA) composite by assembling HA
50 onto carboxylic group-functionalized carbon NFs and post-treating with acid and thermal
51 processes. SEM images of the CNFs-HA composite displayed a homogenous and porous
52 structure, providing a large electrode surface area for the loading of metalloprotein Cytochrome
53 c (*Cyt c*) in H₂O₂ biodetection.¹¹¹ The CNFs-HA composite ECBS obtained better performance
54
55
56
57
58
59
60

1
2
3 than previously documented *Cyt c* loaded biosensors, displaying good analytical performance
4 (linear detection range from 2 μM - 8.7 μM , limit of detection of 0.3 μM) facilitated by a *Cyt*
5
6
7
8 *c* loading capacity that was double that of traditional CNT loading capacities.¹¹¹
9

10 Mondal et al.³⁸ recently reported a facile method for fabricating functional micro-,
11 submicro-, and nano-channels embedded in porous carbon film ECBSs. The microfluidic
12 platform was constructed by electrospinning a skin layer of poly(methyl methacrylate) solution
13 on a silicon wafer substrate, followed by a spin coating of polyacrylonitrile. Thermally-induced
14 carbonization of the composite film decomposed the poly(methyl methacrylate) NFs,
15 producing embedded microchannels in the polyacrylonitrile-derived amorphous monolithic
16 carbon electrode. Pt nanoparticles were then *in situ* assembled on the embedded channels by
17 thermal decomposition of a precursor salt to enhance the performance of the carbon electrode.³⁸
18 Further plasma treatment functionalized the composite surface with carboxylic groups,
19 allowing anti-aflatoxinB1 (anti-AFB1) antibodies to be grafted by carbodiimide-mediated
20 conjugation routes.³⁸ An improved ECBS performance was obtained, attributable to aligned
21 nanochannels in the porous carbon film which simultaneously acted as a reaction chamber for
22 antigen-antibody interactions and a fast electron transport route between the electrolyte and
23 working electrode. The synthesized immunosensor had a higher detection range than
24 previously reported AFB1 sensors and a comparable picomolar limit of detection. Even though
25 the proposed immunosensor was produced for the detection of AFB1 (prevalent in the food-
26 processing industry), synthesizing antigen-immobilized ESNFs with microfabricated channels
27 represents a novel success in the development in state-of-the-art microfluidic devices.¹¹²⁻¹¹⁴
28 Incorporation of microfluidic channels into the porous carbon film serves to improve the
29 sensitivity, stability, and reproducibility of the immunosensor by maintaining the anti-AFB1
30 functionality.¹¹⁵ This result appears analogous to the discussion of Tripathy and co-workers'
31 report (see *section 4.3.1.1.1*). This synthetic route could be extended to the development of a
32
33
34
35
36
37
38
39
40
41
42
43
44
45
46
47
48
49
50
51
52
53
54
55
56
57
58
59
60

1
2
3 broad range of cancer-detecting biosensors by modifying the immobilization and
4 functionalization protocols. According to the literature, the four areas in cancer diagnostics in
5
6 which microfluidic-hybridized-ESNFs may change the current paradigm are: (1) Molecular-
7
8 scale diagnostics; (2) Tumor biology; (3) High-volume screening for therapeutics; and (4)
9
10 Cancer cell isolation.¹¹⁴ The microfluidics field is a rapidly expanding area in cancer detection,
11
12 and there are already instances of approved diagnostic applications.¹¹⁶ A particularly active
13
14 research group in this regard is the team of Prof. Hsian-Rong, who developed multiple
15
16 generations of “NanoVelcro” cell-affinity substrates, in which circulating tumor cell (CTC)
17
18 capture agent-coated nanostructured substrates were utilized to immobilize CTCs with high
19
20 efficiency.^{117,118} Guarino and Ambrosio provide an extensive review on the role of
21
22 microfluidics and ESNFs in the future of cancer diagnostics.¹¹⁴ Integration of these
23
24 technologies represents an innovative platform for fabricating complex nanoscale systems as
25
26 *in vitro* models for toxicological investigation; however, its adoption as a primary diagnostic
27
28 tool remains a largely unknown proposition to-date.¹¹⁶
29
30
31
32
33
34
35
36
37

38 **4.3.1.2.3. Hollow Morphology**

39
40 Ji et al.¹¹⁹ fabricated cationic polyelectrolyte-doped hollow NFs by coaxially
41
42 electrospinning a core/shell solution of poly(allylamine hydrochloride) (PAH) / polyurethane
43
44 (PU) using a specially designed two-capillary spinneret; the spinneret was designed such that
45
46 *in situ* encapsulation of bioactive molecules prevents them from being contacted by the organic
47
48 solvent. Doping of PAH on the PU ESNF allowed *Candida antarctica* lipase B and glucose
49
50 oxidase enzymes to be precisely grafted in spatially isolated compartments on the ESNF
51
52 surface and lumen by ion-exchange interactions between the charged enzymes and ionizable
53
54 groups on PAH, producing woven-membrane NFs with enhanced enzymatic stability. The
55
56 multienzyme ESNF system has good potential for being employed as an ultrasensitive cancer
57
58
59
60

1
2
3 biosensor, assuming transducing elements can be successfully incorporated into the
4 structure. Enzyme biomarker irregularities in certain cancers (i.e., overexpressed ITIH4 (Inter-
5 alpha-Trypsin Inhibitor Heavy chain family member 4) and underexpressed apolipoprotein A1
6 in ovarian cancers)⁶⁹ could be independently targeted using a single ESNF platform, whereby
7 multienzyme cascade reactions *in vivo* could provide an unsurpassed efficiency/specificity for
8 biosensors monitoring cancer progression. The complexity involved in constructing a
9 multienzyme system that simultaneously inhibits negative interferences between grafted
10 enzymes and performs multistep biotransformations might prove too complex for constructing
11 a feasible biosensor. Nevertheless, if multiple enzymes could simultaneously be targeted, it
12 would improve the diagnostic value of the biosensor as a single biomarker can be indicative of
13 a variety of different cancers.
14
15
16
17
18
19
20
21
22
23
24
25
26
27
28
29
30

31 **4.3.2. Optical Biosensors**

32
33 Optical biosensors (OBSs) use light-based sensing methods that measure changes in
34 specific wavelengths of light, which are converted into an electrical readout. Most
35 commercialized platforms use fluorescence labels as the detection system; however,
36 interferometry and spectroscopy of optical waveguides and surface plasmons resonance are
37 also available ¹²⁰. The signal readout instrumentation is usually expensive relative to ECBSs,
38 so their employment in cancer biosensing is relegated to predominantly laboratory-based
39 testing rather than point-of-care devices for *in vivo* analysis ¹². OBSs have been used to detect
40 cancerous analytes such as CEA,¹²¹ PSA,¹²² volatile organic compounds,¹²³ and histamine (for
41 breast, colon, and pancreatic cancers).¹²⁴
42
43
44
45
46
47
48
49
50
51
52
53

54 ESNF-OBSs appear to be particularly useful in detecting early-stage lung cancers.
55 Considering that lung cancer has one of the greatest mortality rates of all known cancers,¹²⁵
56 early diagnosis is of paramount importance to avoid metastasis. Davis et al.¹²³ demonstrated a
57
58
59
60

1
2
3 novel dual-mode optical sensing platform for volatile organic compound differentiation.
4
5 Polydiacetylene (PDA)-embedded ESNFs were produced by mixing a diacetylene monomer
6
7 solution with an acidic solution for 60 minutes. The resultant sol-gel was electrospun at a rate
8
9 of 0.1 - 1.0 mL h⁻¹, subject to an 8 - 20 kV electric field, towards a grounded aluminum plate
10
11 (tip-to-collector distance: 10 - 12 cm). For fluorescence measurements, a poly(ethylene oxide)
12
13 matrix polymer was used to construct PDA-embedded NFs, which were subsequently
14
15 photopolymerized under UV irradiation to produce fluorescence responsive ESNFs. The
16
17 solvent-dependent fluorescent transition of NFs generated a response pattern that was
18
19 successfully used to distinguish between four different organic vapors (THF, chloroform,
20
21 methanol, and hexane). It was further shown that the fluorescent and colorimetric sensing of
22
23 biotin-avidin interactions could be realized by embedding biotinylated-pentacosadiynoic acid
24
25 monomers into silica-reinforced nonwoven NF mats. There is a possibility to broaden the
26
27 application to different cancer monitoring by generalizing the detection response to hapten
28
29 bioconjugate interactions (see **Table 4**). Finally, a three-component PDA NF sensor array was
30
31 fabricated and tested against eight different organic amine vapors. Using colorimetry and
32
33 principal component analysis, analyte-dependent colorimetric responses were observed
34
35 (attributable to amine specific basicity and steric hindrance). This result is particularly useful
36
37 in lung cancer detection as two of the amine vapors tested were piperidine and pyridine, a class
38
39 of aromatic amines. Human exhaled breath contains hundreds of volatile organic compounds,
40
41 and aromatic amines are known biomarkers used to *predict* lung cancer.¹⁹ The sensor array
42
43 differentiated between the eight amine vapors in 72 different samplings, all within a 95 %
44
45 confidence interval.¹⁹ Ultrasensitive detection and differentiation of volatile organic
46
47 compounds that are indicative of onset lung cancers prove to be a very promising platform for
48
49 early lung cancer detection, suggesting the OBS proposed by Davis et al.¹²³ could be employed
50
51 as a novel biosensor that utilizes the technique of electrospinning.
52
53
54
55
56
57
58
59
60

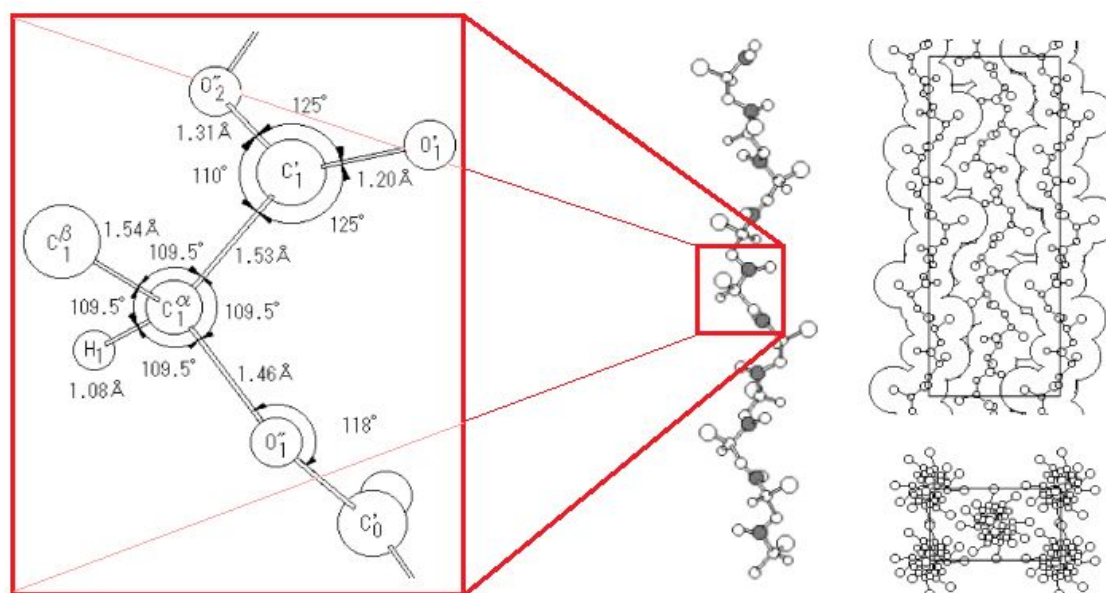
1
2
3 Similarly, Ifegwu et al.¹²⁶ fabricated nylon 6 NFs doped with Au nanoparticles for the
4 colorimetric probe of 1-hydroxypyrene, a biomarker associated with the largest class of cancer-
5 causing compounds: polycyclic aromatic hydrocarbons. Au nanoparticles were *in situ*
6 embedded by chemisorption between the Au nanoparticles and the amide groups on the nylon-6
7 backbone.¹²⁶ The nylon-6 / Au nanocomposite was electrospun to form uniformly dispersed
8 nanoparticle-doped NFs.¹²⁶ A prominent spectroscopic feature of Au nanoparticles is surface
9 plasmons resonance, which arises from the collective oscillatory behavior of Au's free
10 electrons of the conduction band that prompts an intense absorption band in the visible
11 spectrum.¹²⁶ As such, the resultant ESNF was characterized by a highly sensitive, photostable
12 reddish-white fiber that turned blue/purple when in contact with a standard solution of 1-
13 hydroxypyrene.¹²⁶ Au nanoparticles have also been functionalized with DNA and grafted onto
14 ESNFs for detecting nucleic acid-based marker, which are used to monitor not only lung
15 cancers, but also neck, brain, colon, and breast cancers.¹²⁷ Wang et al.¹²⁷ introduced a facile
16 approach to fabricating a novel nanocomposite membrane for highly specific and sensitive
17 detection of nucleic acids. DNA-functionalized Au nanoparticles were assembled on cellulose
18 acetate ESNFs to be used as a fluorescent platform which was highly sensitive, selective, and
19 reproducible, as well as low-cost to fabricate.¹²⁷ Further to fluorescent and colorimetric
20 sampling, Au-labelled targeting molecules can be used as high-contrast agents to visualize
21 injected substances in cells or tissue sections.⁷⁵ Detection of such Au nanoparticle conjugates
22 is particularly effective by electron microscopy, as individual particles can be precisely
23 imaged.⁷⁵ To that end, Au nanoparticles have been used previously as theranostic agents
24 (simultaneous diagnosis and treatment) in photothermal therapy, where irradiation of Au
25 nanoparticles incorporated in as-spun NFs causes them to heat up due to Au nanoparticles
26 absorbing photon energy. The small size and rapid heating of Au nanoparticles, as well as the
27 ability to precisely monitor their locations, provides the necessary framework for selective
28
29
30
31
32
33
34
35
36
37
38
39
40
41
42
43
44
45
46
47
48
49
50
51
52
53
54
55
56
57
58
59
60

1
2
3 heating and destruction of neoplastic cells without damaging the surrounding healthy tissue.¹⁰
4
5 Photothermal treatment by shortwave radiofrequency ablation could be applied with Au
6
7 microelectrodes to penetrate deep-seated tumors, noninvasively.¹²⁸ However, its employment
8
9 as a theranostic agent suggests that non-enzymatic bioreceptors would be required, as high-
10
11 temperature Au nanoparticle-doped ESNFs would likely denaturize any biological components
12
13 immobilized on the surface.
14
15

16 17 18 19 **4.3.3. Mass-Based Biosensors**

20
21 Mass-based biosensors (MBBSs) utilize piezoelectric techniques, where crystals produce
22
23 readout signals based on differential mass measurements that arise from the application of a
24
25 potential force.¹² Immunosensors and microcantilever sensors that adopt piezoelectric
26
27 technology are designed to detect cancerous analytes by immobilizing the appropriate
28
29 conjugate on a sensor chip.¹²⁰ Electrospinning has been used previously to fabricate
30
31 piezoelectric materials for biomedical application, including polyvinylidene polymer NFs
32
33 embedded with barium titanate nanoparticles¹²⁹ and poly(vinylidene fluoride) / PAN-based
34
35 superior hydrophobic piezoelectric solids derived by aligned MWCNTs.¹³⁰ Recently, Zhao et
36
37 al.¹³¹ demonstrated that poly(L-lactic acid) (PLLA) NFs can display piezoelectric properties
38
39 along their diameter fiber direction, where previously documented PLLA MBBSs¹³² were only
40
41 able to obtain shear-direction piezoelectricity. The authors attribute this success to the twisting
42
43 of C=O dipoles in the polymer chains along the shear fiber direction, which was obtained by
44
45 generating a high DC electric field and applying it to the polymer melt during
46
47 electrospinning.¹³¹ Typically, the helical conformation structure of PLLA orients the dipole
48
49 components perpendicular to the fiber chain direction, such that adjacent polymer chains will
50
51 be arranged antiparallel to each other, shown in **Figure 7**.¹³³ This results in a configuration that
52
53 does not permit piezoelectricity along the fiber diameter direction. By applying shear force and
54
55
56
57
58
59
60

1
2
3 a strong electric field in the same direction, Zhao et al.¹³¹ were able to align the C=O dipoles
4 along the polymer chain and induce piezoelectricity across the fiber diameter.¹³¹ The ESNFs
5 were further functionalized with two Au electrodes after being hot-pressed for 30 minutes at
6 50 MPa, from which supercritical CO₂ post-treatment produced a PLLA ESNF with 61.8%
7 crystallinity.¹³¹ An output current and voltage of 8 pA and 20 mV, respectively, was obtained
8 by a simple push-release response to an applied force perpendicular to the fiber length.¹³¹ It is
9 stated that this device enables a broad range of promising future applications in the field of
10 biosensing.¹³¹ It is possible to consider adapting the push-release response to detecting surface
11 stresses induced by bioreceptor-analyte specific binding. A NF mat woven using this process
12 could produce a highly sensitive MBBS with a very high surface area, corresponding to a
13 greater bioreceptor immobilizing capacity. Intuitively, a high concentration of grafted
14 bioreceptors interacting with target analytes would result in an output response proportional to
15 the number of bound target analytes, perhaps validating it as a novel biosensor platform for
16 cancer detection. More experimental effort is required to corroborate this remark.



36
37
38
39
40
41
42
43
44
45
46
47
48
49
50
51
52
53
54
55
56
57
58
59
60

Figure 7. Poly(L-lactic acid) (PLLA) Nanofiber. **(Left)** Molecular geometry of PLLA. **(Middle)** Helical structure of PLLA, where shadowed circles denote carbonyl carbon atoms, and outer large circles denote the methyl groups. **(Right)** Crystal structure of the α -form of

1
2
3 PLLA with top and profile projections. Adapted for reprint with permission from ref 133.

4
5
6 Copyright 2003 American Chemical Society.

7 8 **4.3.4. Calorimetric Biosensors**

9
10 Calorimetric Biosensors (CBSs) measure changes in heat from enzymatic exothermic
11 reactions, which can be used to measure analyte concentrations.¹² There are very few instances
12 in literature where CBSs are used in cancer diagnostics; fewer still, ones that utilize the
13 technique of electrospinning. However, an ESNF-CBS with cancer-detecting potential was
14 recently reported by Gonzalez and Frey.¹³⁴ Poly(vinyl caprolactam) (PVCL) was
15 copolymerized with hydroxymethyl acrylamide (NMA), after which it was electrospun and
16 thermally cured to produce P(VCL-*co*-NMA) temperature-responsive chemical hydrogel NFs.
17 The temperature response was measured using a swelling-shrinking experiment, and all
18 samples responded quickly and reversibly to changes in temperature.¹³⁴ This unique property
19 may be utilized more in the future, presuming nanotechnology continues to mature.
20
21
22
23
24
25
26
27
28
29
30
31
32
33
34
35
36

37 **5. DRUG DELIVERY SYSTEMS USING ELECTROSPUN NANOFIBERS**

38
39 Size variations within the nanoscale enable nanoparticles – functionalized, or not, with
40 conjugated biomolecules for specific intracellular targeting – to be introduced into the body
41 with varying bioavailability and blood circulation times.¹³⁵ It has been demonstrated that
42 nanoparticles with diameters less than 10 nm are removed from the body by extravasation and
43 renal clearance,¹³⁶ nanoparticles with diameters greater than 200 nm are typically removed by
44 phagocytes,¹⁰ and nanoparticles between 10 nm and 100 nm can penetrate small capillaries,⁹
45 be sequestered in endocytic vesicles,^{137,138} and circulate for prolonged periods of time,
46 suggesting optimal nanoparticle diameters fall between 10 nm and 100 nm in size.^{139,140} The
47 delivery vehicle for parenteral administration of these nanoparticles is typically a liposomal or
48 polymeric carrier.⁹ While liposome assisted drug delivery has been the subject of a plethora of
49
50
51
52
53
54
55
56
57
58
59
60

1
2
3 positive results in preclinical trials, clinical translation has progressed moderately due to
4
5 problems with industrial scalability, post-modification functionality, pharmacokinetic
6
7 evaluation, and release profile moderation.¹⁴¹ In contrast, polymeric DDSs are capable of
8
9 controlled and sustained release of therapeutic agents as the biochemical properties of
10
11 encapsulation systems are optimized according to the release profile needed for a given target
12
13 tissue.¹⁴² An ideal universal drug-delivery platform is not likely to be obtained, however
14
15 polymeric DDSs represent a promising pre-requisite for future generation DDSs which might
16
17 incorporate combinatorial biosensing feedback as well as *in vivo* release of cytotoxic treatment.
18
19 As such, ESNF DDSs will be critically reviewed in their biomedical context.
20
21
22
23

24 ESNFs may be fabricated as implantable DDSs for cancer therapeutics, analogous in
25
26 principle to the synthetic methodology employed in ESNF biosensors. Morphological
27
28 properties of ESNFs saturated with cytotoxic agents contribute significantly to drug release
29
30 kinetics.²⁷ ESNFs with a high surface-area-to-volume ratio can accelerate the dissolution of
31
32 therapeutic agents in an aqueous environment, enhancing the drug release efficiency in
33
34 localized tumors.^{16,143} For this reason, most examples of ESNF-DDSs practice coaxial
35
36 electrospinning to obtain core-shell or hollow NFs (see **Table 2**). Further to ESNF
37
38 morphologies, drug release profiles have been shown to be controlled by the composition and
39
40 concentration of shell polymers, solvents used, drug/protein concentration, surface additives,
41
42 electrospinning conditions, and the solubility characteristics of bioactive agents.⁵⁹ Therapeutic
43
44 agents in an electrospun matrix rely on the surrounding fluid to permeate into the scaffold in
45
46 order to dissolve it so that it can be released by either a diffusion, leaching, or combinatorial
47
48 mechanism. The rate at which drugs are released *in vivo* depends on the pharmacokinetics once
49
50 they are incorporated within NFs; to mediate tumor area-specific release, drug-polymer process
51
52 parameters can be selected to optimize the release kinetics indirectly. ESNFs that are
53
54 biodegradable and biocompatible have become the new tendency due to their dual-use in DDSs
55
56
57
58
59
60

1
2
3 and in implantable scaffolds.¹⁹ In contrast to non-biodegradable polymers, in which the drug-
4
5 diffusion distance is dependent on a fixed geometry, drug-diffusion in biodegradable polymers
6
7 is a function of the polymer degradation rate, introducing another order of complexity to the
8
9 fabrication process.¹⁴⁴ So far, popular biodegradable electrospinnable polymers identified in
10
11 the literature are polycaprolactone, polyvinyl alcohol, cellulose acetate, gelatin and zein
12
13 protein.²⁸ Generally, natural polymers (such as cellulose acetate, gelatin, and zein protein) are
14
15 the best choice for biocompatibility as they facilitate cell attachment / cellular activity and
16
17 possess functional groups compatible for hydrophilic interactions; this is especially appropriate
18
19 if the therapeutic agent is bioactive in nature. Considering most instances of sustained drug
20
21 release are reported for small hydrophobic drugs or large biological macromolecules, chemical
22
23 and thermal modifications can destabilize the desired physiological properties.⁵¹ In this respect,
24
25 care must be taken to achieve designs of considerable utility.
26
27
28
29
30
31
32

33 **5.1. Modes of Delivery for Electrospun Nanofibers**

34
35

36 A common approach employed for the delivery of ESNF drug-loaded systems is through
37
38 the oral,²⁰ buccal¹⁴⁵ and sublingual²² routes; where the drug is rapidly metabolized in the oral
39
40 cavity. A range of hydrophilic polymers can be appropriate for the development of such
41
42 systems, including poly(vinyl alcohol) (PVA),²⁰ poly(vinyl pyrrolidone) (PVP)¹⁴⁶ and
43
44 poly(ethylene oxide) (PEO)¹⁴⁷.
45
46
47

48 Through the transdermal route, drugs are administered and delivered locally or
49
50 systematically via the skin. Transdermal drug delivery is a desired alternative to oral delivery,
51
52 which can be advantageous over hypodermal injections, as a less invasive alternative.²³ This
53
54 approach is of interest for drug-loaded systems that cannot be taken up by the oral route due to
55
56 rapid enzymatic gastrointestinal and hepatic pre-systemic metabolism.¹⁴⁸ Due to the nano-
57
58 dimensions and the high-surface-to-volume ratio of the ESNFs, good dispersity of the drug on
59
60

1
2
3 the polymer matrix can be achieved, significantly increasing the solubility of the drug at the
4 surface of the skin.¹⁴⁹
5
6
7

8 The ocular route is a minimally-invasive approach of targeted delivery of ESNFs through
9 the ocular tissues. Aside from the direct delivery path, such an approach carries disadvantages
10 due to the need of semi-transparent membranes, difficulties in application, and potential
11 contaminations. Nonetheless, the usage of ESNF as a topical system for the delivery of
12 substances can be beneficial in comparison to eye drops where less than 5% of the contained
13 drug reaches the desired tissue.¹⁵⁰
14
15
16
17
18
19
20
21

22 In a more direct approach, anti-cancer ESNF scaffolds can be placed on the tumor bed for
23 systemic localized delivery.¹⁵¹ Because the majority of the ESNFs follow a passive diffusion
24 release behavior, thus lacking the ability of controlling the need of reaching the desired
25 substance concentration for effective killing of the cancer cells, stimuli-responsive (pH-
26 dependent, photothermal or magnetic trigger of drug release) smart drug delivery ESNFs with
27 on-demand drug release capabilities have attracted much attention.¹⁵² Chemotherapeutic in-
28 stent devices consisting of an ESNF surface that can be surgically placed at the tumor-bearing
29 area in cancers, such as ureter¹⁵³ or colorectal¹⁵⁴ cancer, is another approach that can provide
30 systemic drug release of anticancer drugs along with providing the required mechanical
31 stability to prevent restenosis caused by tumor ingrowth.¹⁵⁴
32
33
34
35
36
37
38
39
40
41
42
43
44
45
46
47

48 **5.2. Release Behavior of Drug-Loaded Electrospun Nanofibers**

49

50 The solvent-drug and polymer-drug compatibilities are particularly noteworthy interactions
51 in controlling drug release rates, so detailed strategies have been outlined in the literature¹⁴⁴ for
52 pairing solvents compatible with polymers to mitigate phase separation of drug-loaded ESNFs
53 (which can result in a burst release of therapeutic agents upon dissolution). In short, to achieve
54 a high drug loading efficiency, hydrophilic drugs are paired with hydrophilic ESNFs, and
55
56
57
58
59
60

1
2
3 hydrophobic drugs with hydrophobic ESNFs.⁵⁹ A strategy adopted by many authors requires
4
5 blending polymers with both hydrophobic- and hydrophilic-moieties, which further helps
6
7 diversify the drug loading range of ESNFs.⁵⁹ By utilizing the high surface areas of coaxially
8
9 spun hollow and/or core-shell NFs with multiple therapeutic agents, one could not only
10
11 incorporate multiple stimulants in a single therapeutic platform but also tailor the release of
12
13 each agent independently by altering the fiber thickness and localization ²⁸. It has been
14
15 remarked that these morphologies also provide the additional benefit of inhibiting the initial
16
17 burst release response.³⁷
18
19
20
21

22 For instance, Bonadies *et al.*¹⁵⁵ developed new drug administration systems from
23
24 poly(butylene adipate/poly(vinylpyrrolidone) core/shell ESNFs for malaria and prostate cancer
25
26 applications. A considerable burst release was observed in polymer blends with a greater drug-
27
28 to-poly(vinylpyrrolidone) ratio; this is characteristic of hydrophilic shell-polymers accelerating
29
30 hydrophobic drug solubilization upon immersion in an aqueous environment.¹⁵⁵ Subsequent
31
32 diffusion from the hydrophobic core-polymer – and the low solubility of the anti-malarial drug
33
34 – resulted in the sustained release of remaining treatment at a controlled rate.¹⁵⁵ Polymer blends
35
36 with a lower drug-to-poly(vinylpyrrolidone) ratio performed the best for *in vitro* inhibition of
37
38 malarial parasites, and furthermore reduced the viability of prostatic cancer cell.¹⁵⁵
39
40 Ramachandran *et al.*¹⁵⁶ developed a flexible theranostic implantable system for prolonged and
41
42 sustained (30 days, zero-order) release of Temozolomide, an anti-glioma chemotherapeutic
43
44 drug, under *in vivo* conditions, using a rat model. Different sets of co-axial ESNFs were
45
46 produced to achieve fiber-by-fiber switching between specific time periods.¹⁵⁶ The rat model
47
48 illustrated a constant drug release of 116.6 $\mu\text{g}/\text{day}$ with only a very small amount of drug
49
50 leakage in the peripheral blood (<100 ng), rendering a long-term (>4 months) survival rate of
51
52 85.7%.¹⁵⁶ Similarly, G. Xia *et al.*¹⁵¹ developed a Gemcitabine (GEM)-based implantable
53
54 system against pancreatic ductal adenocarcinoma in BALB/c athymic mice. The system
55
56
57
58
59
60

1
 2
 3 consisted of GEM dispersed in hyaluronic acid (HA) hydrosol (forming the sol solution)
 4
 5 enwrapped with PLA-HA (electrospinning solution) to form core-shell (GEM@PLA-HA)
 6
 7 ESNFs via sol-electrospinning. Although the antitumor effect of the developed system was not
 8
 9 superior to that of GEM intravenous administration, due to the localized approach the mice
 10
 11 implemented with the GEM@PLA-HA ESNFs presented a more efficient inhibition of residual
 12
 13 tumor growth and a significantly reduced liver toxicity. Such a system could be implanted upon
 14
 15 tumor removal for the prevention of tumor reoccurrence locally.¹⁵¹ Earlier this year, Hyun Mu
 16
 17 et al.¹⁵⁷ developed an injectable short PLA cytokine immobilized (Cyto-sPLA) system. The
 18
 19 Cyto-PLA nanofibrous mats were produced via electrospinning. The produced ESNFS were
 20
 21 then dispensed in ethanol, microtomed, and filtered to obtained Cyto-sPLA ESNFs with length
 22
 23 ranging from 15-100 μm . Ethanol-based aqueous solutions consisting of polydopamine (pDA)
 24
 25 conjugated IL-2 Fc immobilized Cyto-sPLA ESNFs were injected near the targeted tumor site
 26
 27 in mice. The treated mice presented a significantly increased number and proportion of CD8+
 28
 29 T cells for up to 9 days, presenting retarded tumor progression with an up to 70% tumor
 30
 31 regression.¹⁵⁷ This is an innovative immunotherapeutic approach towards the reinvigoration of
 32
 33 the body's non-functional CD8+ cells for suppressing tumor growth.¹⁵⁷ The results of these
 34
 35 studies suggest a facile approach for the design of nanoscale targeted drug administration,
 36
 37 while simultaneously validating nanofibrous assemblies as potential replacements to traditional
 38
 39 therapeutics.
 40
 41
 42
 43
 44
 45
 46
 47
 48
 49
 50

Table 5. Different drug release mechanisms.¹⁵⁸

Release exponent (n)	Drug Transport Mechanism	Rate as a function of time
≤ 0.45	Fickian Diffusion	$t^{-0.5}$
$0.45 < n < 0.89$	Non-Fickian (Kinetic) Transport	$t^{(n-1)}$

0.89	Case II Transport*	Zero order release
> 0.89	Super Case II Transport**	$t^{(n-1)}$

*drug release is constant and controlled by polymer relaxation

**drug release is polymer erosion-controlled

Characterizing the drug pharmacokinetics in ESNFs is difficult due to the complex morphologies of these polymer matrices and the structural variations they may undergo due to swelling. Various mathematical models have been proposed to describe drug release kinetics including first order models, the Higuchi model, the Hixson-Crowell model, and the Korsmeyer-Peppas model. Good success has been achieved in the Korsmeyer-Peppas framework, which models the release kinetics as a general power-law derived from a polymeric system, and can be modified to compensate for burst-release responses¹⁵⁸:

$$\frac{M_t}{M_\infty} = K_{kp} t^n \quad (1)$$

Where M_t is the amount of drug released in time t , M_∞ is the amount of drug released after time ∞ , n is the diffusional exponent or drug release exponent, and K_{kp} is the Korsmeyer release constant.

Release kinetics are evaluated using the logarithmic form of equation 1¹⁵⁸ :

$$\log\left(\frac{M_t}{M_\infty}\right) = \log(K_{kp}) + n \log(t) \quad (2)$$

By plotting $\log(M_t/M_\infty)$ against $\log(t)$, a linear plot with a gradient of n and an intercept of $\log(K_{kp})$ may be obtained. To determine whether the mechanism occurs by diffusion, leaching, or a combination of the two, the exponent variable n is used to describe drug release in cylindrical shaped matrices (and occasionally thin films)²⁸. **Table 5** provides the mechanism boundaries.

If the release mechanism does not conform to the application, the ESNF-drug matrix has been designed for (such as a reservoir-type therapeutic device exhibiting Case II transport as opposed to Fickian diffusion) then process parameters (such as applied voltage or polymer supply rate) may be adjusted to alter the fiber architecture. Various modified forms of equation 1-1 have appeared in previous drug release studies, given in **Table 6**.

Table 6. Strategies for sustained drug release from ESNFs.

Fiber System	Agent	Release (%)				Release Model	Ref.	
		Name	Loading (wt. %)	1 h	24 h			7 d
PCL:PVA	Metoclopramide hydrochloride	1	5	55	65	68	$M_t = \left[\frac{2\pi h D \phi C_s}{\ln(r_o/r_i)} \right] t$	159
PLLA:PVA	Metoclopramide hydrochloride	1	2	12	22	25	$M_t = \left[\frac{2\pi h D \phi C_s}{\ln(r_o/r_i)} \right] t$	159
PCL:Gelatin	Metronidazole	33.4	5	60	95	100	$M_t = \left[\frac{2\pi h D \phi C_s}{\ln(r_o/r_i)} \right] t$	160
28%Zein:1%Ferulic Acid	Ketoprofen	10	5	100	-	-	$\frac{M_t}{M_\infty} = K_{kp} t^n$	161
PCL:PLGA	TFV, AZT, RAL	15	12	28	56	-	$\frac{M_t}{M_\infty} = K_{kp} t^n$	162
PCL:PEG	Salicylic acid	10	10	25	40	100	$\frac{M_t}{M_\infty} = \frac{M_b}{M_\infty} + K_{kp} t^n$	163

PCL = Polycaprolactone; PVA = Polyvinyl alcohol; PLLA = Poly(L-lactic acid) PEG = Polyethylene glycol; PLGA = Poly(lactic-co-glycolic) acid; TFV = Tenofovir; AZT = azidothymidine; RAL = Raltegravir. M_t is the amount of drug released at time t, M_∞ is the amount of drug released at time ∞ , M_b is the burst release, K_{kp} is the Korsmeyer release constant, n is the diffusional exponent or drug release exponent, h is the height of the cylinder,

1
2
3 r_o is the outside radius of the fiber, r_i is the inside radius of the fiber, D is the diffusion
4 coefficient, φ is the partition coefficient for the drug from the core to the shell, C_s is the steady
5 state concentration.
6
7
8
9

10
11 The number of interrelated parameters affecting the release kinetics makes it difficult
12 to provide any meaningful comparisons between the isolated studies listed in **Table 6**. Note,
13 however, the difference in release rates between the PCL:PVA and PLLA:PVA fibers, keeping
14 all other variables constant. Over twice as much metoclopramide hydrochloride is released
15 from the PCL:PVA fiber compared to the PLLA:PVA fiber after 14 days. The authors attribute
16 this observation to a far higher porosity in the PCL shell, which allowed direct access to the
17 drug by the surrounding fluid, resulting in a predominantly burst release mechanism. On the
18 contrary, the PLLA shell exhibited a fickian diffusion mechanism. This is but one example of
19 many, yet it reflects the importance of material selection in mediating tumor-specific release
20 of cytotoxic treatment. The PLLA:PVA fiber is more relevant in the context of ESNF-DDSs;
21 reservoir-type DDSs have been applied to the treatment of breast,¹⁶⁴ colorectal, lung, head,
22 neck,¹⁶⁵ and many more cancers. PLLA:PVA would be particularly good in the treatment of
23 deep-seated tumors due to both PLLA and PVA being biodegradable, meaning prolonged *in*
24 *vivo* treatment can be obtained without the need to remove the polymer matrix by operation
25 once the treatment period is complete.
26
27
28
29
30
31
32
33
34
35
36
37
38
39
40
41
42
43
44
45
46
47
48
49

50 **5.3. The Current and Future Status of Drug-Loaded Electrospun Nanofibers**

51
52 In the absence of approved alternative treatment methods, traditional therapeutic practices
53 have been the focus of some practical reform. Similar to the novel therapeutic platforms
54 highlighted in this review, systemic chemotherapeutic drugs have, quite unsuccessfully,
55 endeavored at improved delivery efficiencies by incorporating cancer-targeting moiety. A
56
57
58
59
60

1
2
3 median of only 0.7% of injected chemotherapeutic agents reach solid tumors upon systemic
4 administration, according to a recent 10-year long literature survey.¹⁶⁶ Some instances of
5 improved systemic treatment have been reported using combinatorial chemotherapy and
6 photodynamic therapy nanohybrids¹⁶⁷ or synergistic nanoparticle / chemotherapeutic drug
7 hybrids¹⁶⁸; however, interest has shifted to local rather than systemic administration methods.
8 Naturally, there is an ongoing effort to not only clinically approve various novel therapeutic
9 agents, for example, those listed in **Table 7**, but also to optimize their delivery platform for
10 routine clinical application, like those listed in **Table 8**. Optimized delivery platforms may
11 mitigate the current problems with systemic administration; however, several problems remain
12 before ESNF DDSs transition to clinical trials. The essential ones are 1) secondary removal
13 surgery of non-biodegradable scaffolds; 2) the potential hazard of residual solvent from the
14 manufacturing process; and 3) the biological challenge of foreign-body administration.¹⁶⁵ Of
15 note is the complexity surrounding the third point, which was briefly discussed in *Section 1*
16 and *Section 3*. It is one of the major objectives in site-specific delivery to overcome the
17 biological barriers that preclude efficacious unloading of cytotoxic treatment which, currently,
18 is a non-trivial yet surmountable task. As the mechanisms involved in hindering drug delivery
19 become better understood, functional ESNF DDSs outside the confines of convention may be
20 formulated to address these limitations.¹⁶⁹ For instance, active-targeting micelles have been
21 encapsulated in core/shell NFs by coaxially electrospinning micelle-doped-poly(vinyl alcohol)
22 / cross-linked gelatin. Compared to the traditional administration of micelles for cancer
23 therapy, the implantable doxorubicin-micelle-loaded NF reduced the frequency of
24 administration while retaining high efficacy against solid tumors.¹⁷⁰ More recently, an
25 implantable hierarchical-structured fiber device developed via microfluidic-electrospinning
26 was capable of co-delivering Doxorubicin (DOX)-loaded micelles encapsulated within ESNFs
27 synergistically with the tyrosine kinase inhibitor, apatinib (AP), loaded into the ENSF's
28
29
30
31
32
33
34
35
36
37
38
39
40
41
42
43
44
45
46
47
48
49
50
51
52
53
54
55
56
57
58
59
60

1
2
3 matrix.¹⁷¹ This system aimed to inhibit P-glycoprotein (P-gp), an ATP-dependent efflux pump
4
5 by preventing the over-expression of the protein aiming to overcome multiple drug resistance
6
7 (MDR). The device was implanted to nude mice bearing multidrug-resistant human mammary
8
9 adenocarcinoma (MCF-7/Adr) tumors. The sustained release of AP continuously inhibited the
10
11 P-gp efflux pump, allowing for an increased intracellular uptake of DOX. The system presented
12
13 low systemic toxicity and significantly decreased tumor volumes in comparison to the single
14
15 drug ESNFs and the intravenously injected mice.¹⁷¹
16
17
18

19
20 These active targeting approaches enhance the specificity of encapsulated cargo to
21
22 diseased tissues, minimizing deposition in non-target locations. However, the apparent
23
24 therapeutic superiority of active-targeting approaches over non-targeting approaches is still a
25
26 matter of some debate, with somewhat paradoxical results being reported in the literature.¹⁷²
27
28 Several studies have reported an improved efficacy and uptake of ligand-targeted therapeutics
29
30 in neoplastic cells relative to their non-targeted analogs,^{170,173,174} while conversely there are
31
32 studies that report no improvement in bioavailability of ligand-targeted therapeutics at tumor
33
34 sites.¹⁷⁵ This is perhaps a contributing factor as to why only one active-targeting nanomedicine,
35
36 Ontak®, has been FDA-approved (as of 2016).^{62,176} It is more likely that economical and
37
38 regulatory limitations heavily contribute to the lack of currently-available ESNF DDSs. From
39
40 start to finish, an estimated 10-15 years and \$1 billion worth of pre-clinical / clinical phase
41
42 testing are required before therapeutics become available on the market.⁶² The limitations in
43
44 pharmaceutical development are typically centered on four common trajectories: 1) reliability
45
46 of the marketed product; 2) scalability of the manufacturing process; 3) chemical instability or
47
48 denaturation of therapeutic compounds during manufacturing; and 4) long term stability of
49
50 product after administration.¹⁷⁷ As such, accurate characterization of the polymeric carrier-drug
51
52 matrix is a necessary pre-requisite before predicting its behavior in a biological context. This
53
54 is an important issue if ESNF DDSs are to progress beyond theoretical intrigue.⁶² There are
55
56
57
58
59
60

other significant steps involved in reaching clinical trial phases, but it is out with the scope of this review to highlight them in detail; the reader is referred to references^{62,141,177} for a more comprehensive account.

Table 7. Examples of Nanoparticle-based therapeutics in clinical trial phases.

Therapeutic Agents	Target Cancer	Clinical Trial Phases	Type	Recruitment Status	Trial ID (ClinicalTrials.gov)
Carbon nanoparticle	Rectal Cancer	Not applicable	Lymphatic tracer	Not yet recruiting	NCT03550001
Carbon nanoparticle	Thyroid Cancer	Not applicable	Lymphatic tracer	Completed	NCT02724176
BIND-014, docetaxel nanoparticle	KRAS Mutation Positive or Squamous Cell Non-small Lung Cancer	Phase II	Second-line treatment	Completed	NCT02283320
S-1, Albumin-bound paclitaxel nanoparticle	Advanced Pancreatic Cancer	Phase II	First-line treatment	Active, Not recruiting	NCT02124317
Bevacizumab (biological), gemcitabine hydrochloride (drug), S-1 (drug)	Breast Cancer	Phase II	First-line treatment	Completed	NCT00662129
Paclitaxel albumin-stabilized nanoparticle	Ovarian, Peritoneal Cancers	Phase I	First-line treatment	Completed	NCT00825201
Magnetic nanoparticle	Prostate Cancer	Early Phase I	Treatment	Completed	NCT02033447
CRLX101, enzalutamide	Metastatic Castration Resistant Prostate Cancer	Phase II	First-line hormonal therapy, Treatment	Recruiting	NCT03531827
DOTAP:Chol-fus1 nanoparticle	Lung Cancer	Phase I	Treatment	Recruiting	NCT01455389
EktoTherix™ Tissue Repair Scaffold	Non-melanoma Skin Cancer, Basal Cell Carcinoma, Squamous Cell Carcinoma	Not applicable	Treatment	Completed	NCT02409628

1
2
3
4
5
6 Despite the many benefits that ESNF DDSs boast, a major liability to their adoption as
7
8 primary point-of-care is the initial burst release of drugs upon intravenous administration.⁹ This
9
10 attribute is observed in many diffusion-release ESNF delivery platforms, like some of those
11
12 listed in **Table 8**, which diminishes or undermines the intended application. For example,
13
14 recently Gemcitabine-loaded poly(L-lactate) / hydrosol ESNFs were fabricated by Xia et al¹⁵¹
15
16 for the purpose of pancreatic recurrence prevention. *In vitro* and *in vivo* studies suggest the
17
18 manufactured drug-polymer platform is well suited for abating residual cancerous cell
19
20 proliferation after primary-care surgery. However, initial burst-release of up to 29.8% in the
21
22 first day of loaded Gemcitabine was observed upon administration, with subsequent controlled
23
24 release for up to 3 weeks after. This poses some inherent complications. Firstly, the ESNF
25
26 platform may only be implanted once, which concerns the long-term objective of localized
27
28 treatment, and secondly, this form of treatment cannot significantly increase the concentration
29
30 of therapeutic agents in the blood. The results, while promising, must demonstrate a
31
32 transferable efficacy in humans before progressing to a clinical trial phase. Foremost, the
33
34 remarks of the authors reiterate a common caveat in the literature: secondary removal of the
35
36 ESNF platform is required if it is not biodegradable. The biodegradability component is a
37
38 subject of great interest for localized DDSs. It has been remarked that the continued
39
40 advancement of biodegradable ESNF DDSs might facilitate a more rapid transition of the
41
42 nanotherapeutic field from promising to commonplace,¹⁶⁵ as, indeed, most currently approved
43
44 nanoparticle-loaded platforms consist of simple analogs of well-described approved drugs.⁶²
45
46 From a purely scientific perspective, improvements in the biological understanding of diseased
47
48 states and how they interact with administered ESNF DDSs, along with improvements in
49
50 materials engineering, will serve to expand upon the already encouraging results reported in
51
52 this review and advance nanotherapeutics into commonplace application.
53
54
55
56
57
58
59
60

Table 8. Some examples of promising ESNF DDS platforms.

Therapeutic Agent	Materials and Methods	Drug Release Studies	<i>In vivo</i> studies	<i>In vitro</i> studies	Ref.
Ampicillin	Different concentration of ampicillin were blended with core/shell poly(methyl methacrylate)/nylon6 NFs by coaxial electrospinning	Smooth core/shell fibers encapsulating variable concentrations of ampicillin were obtained, giving a sustained release of non-Fickian diffusion (stage 1), and Fickian diffusion (stage 2 and 3) mechanisms over a 1 month period.	N/A	The antibacterial activity of the system was verified by means of optical density measurements against Gram-positive <i>L. innocua</i> .	178
Acetaminophen	Drug loaded Core/shell poly(vinyl pyrrolidone)/ethyl cellulose NFs were fabricated using a Teflon-coated concentric spinneret in a modified coaxial electrospinning set-up.	Amorphously distributed acetaminophen core-shell NFs with linear morphologies and clear core-shell structures were obtained, exhibiting tunable dual drug controlled-release profiles over a minimum of 24 hours.	N/A	N/A	179
Doxorubicin (DOX)	Core-shell structured NaGdF ₄ Yb/Er@NaGdF ₄ :Yb@mSiO ₂ -polyethylene glycol nanoparticles loaded with the antitumor drug, doxorubicin, were incorporated into poly(ϵ -caprolactone) and gelatin loaded with antiphlogistic drug, indomethacin, to form NFs via electrospinning process.	Burst release of therapeutic agent (60% in the first 15 hours) and subsequent diffusional release (80% cumulative release after 64 hours).	Multifunctional spinning pieces were surgically implanted at the tumor sites of mice as part of orthotopic chemotherapy by controlled-release of Doxorubicin from mesoporous SiO ₂ . The inflammatory response was suppressed, helping wound healing <i>in vivo</i> .	N/A	180
Doxorubicin (DOX)	Graphene	Sustained release of DOX following a	N/A	Cell viability results showed the higher	181

	Oxide / TiO ₂ / DOX composites were loaded into chitosan/poly(lactic acid) (PLA) solutions to fabricate electrospun chitosan / PLA / GO / TiO ₂ / DOX NF scaffolds via electrospinning process.	small burst release was achieved from NF scaffolds with 30 and 50µm thicknesses within two weeks incubation time. The faster DOX release rate from NFs was obtained in pH 5.3 compared to pH 7.4. Korsmayer-Peppas kinetic model was used to determine the DOX release mechanism.		proliferation inhibition effect of NFs on target lung cancer cells in the presence of a magnetic field.	
Mycophenolic acid (MPA)	Coaxial fibers with poly(ε-caprolactone) (PCL)/MPA core and PCL sheath NFs were produced using traditional and coaxial electrospinning techniques	MPA-encapsulated coaxial fibers exhibited sustained release of cytotoxic treatment over a 100-hour period while MPA-incorporated single fibers exhibited burst-release mechanics.	N/A	<i>In vitro</i> glioblastoma multiforme (GBM) tumour cell culture results demonstrated strong cell suppression, with coaxial fibers inhibiting GBM cell growth 3-5x more than single fiber membranes	182
Niflumic acid (NIF)	High throughput production of mats with PVP via nozzle-free electrospinning process. The product was then mixed with microcrystalline cellulose for capsule formulation.	Amorphous NIF was formed. The dissolution rate of the capsule formulation showed a 14-fold increase within the first 15 minutes.	N/A	N/A	143
Temozolomide (TMZ)	TMZ was initially loaded into chitosan nanoparticles and synthesized CS/TMZ nanoparticles were incorporated into the synthesized poly (ε-caprolactone diol) based polyurethane (PCL-Diol-b-PU) NFs using electrospinning techniques	Sustained TMZ release for 30 days with the zero-order kinetic model was achieved from both CS/TMZ loaded PCL-Diol-b-PU and gold-coated NFs	N/A	Cell viability results indicated that the gold-coated NFs can effectively inhibit the growth of U-87 glioblastoma cells	183

6. CONCLUSIONS AND OUTLOOK

Electrospinning has become a valuable means of producing functional ESNFs with unique morphological properties for biosensor and DDS applications. More research is being conducted into understanding the interactions that govern the overall effectiveness of these therapeutic platforms, and technological advancements in the field of nanoscale biomedicine is assisting the transition into localized point-of-care treatment methodologies. Biomarkers and biological analytes provide meaningful information in cancer diagnostics and treatment. However, their low concentration in complex biological media for early-stage cancers requires an ultrasensitive, highly specific, reproducible sensing device. The sensitivities of many ESNF-based biosensors are now mature enough to detect cancerous analytes in bodily fluids, providing the necessary framework for non-invasive sampling. They may be applied routinely as well, outputting accurate results with minimal maintenance and handling expertise; this is in stark contrast to traditional methods of analysis, which are often time-consuming, require trained personnel, and can be very costly. It is without a doubt that ESNF-based biosensors and DDSs are recognized as very promising areas of research in the field of cancer therapeutics, but they currently represent a niche compared to the total pharmaceutical and medical device market.

Many ESNF-based biosensors have been developed and reported in this literature review, utilizing a diverse inventory of polymers and approaches, incorporating or not nanoscale building blocks with pre- or post-treatment processes to produce biosensor platforms with improved analytical performance and functionality. It is challenging to identify which method of detection is the most appropriate, considering the many parameters involved in synthesizing an ESNF-based biosensor. Few biosensors rival the degree of molecular recognition – and the ultra-sensitivities that result – offered by enzymatic ECBSs, however, which is why most biosensors reported in literature rely on this method of transduction. To that end, spatial

1
2
3 architectures of NFs, electrode materials, immobilization techniques, and nanoscale building
4
5 block dispersion strategies have been the object of much experimental effort, all of which can
6
7 be incorporated within an ESNF framework. It is expected that by exploiting the versatility of
8
9 electrospinning, ESNF-based biosensors and DDSs can be expanded to a broader range of
10
11 cancers by immobilizing and maintaining a broader range of bioactive agents. Nevertheless,
12
13 relatively few of these therapeutic platforms have been employed practically, and there are
14
15 currently no commercially available devices. To validate them as primary point-of-care
16
17 sampling and treatment devices, research towards multi-analyte / multi-drug systems is
18
19 required. Simultaneous measurement of cancerous analytes will improve the biosensor's
20
21 diagnostic value, as many overexpressed biomarkers are indicative of a range of cancers.
22
23 Additionally, sequestration of multiple therapeutic agents in a single ESNF matrix can be an
24
25 effective means of inhibiting metastatic tumors, which is important in improving mortality rates
26
27 for cancer patients. Some constraints, such as currently unobtainable economies of scale,
28
29 complex synthetic routes, and legislative limitations have kept ESNF-based biosensors / DDSs
30
31 in pre-clinical and clinical trial stages. Yet, the rate of their development promises that they
32
33 will debut in routine clinical application in the foreseeable future.
34
35
36
37
38
39
40

41 **ABBREVIATION LIST**

42
43
44
45 CBS = Calorimetric Biosensor
46
47 CNT = Carbon Nanotube
48
49 DDS = Drug Delivery System
50
51 ECBS = Electrochemical Biosensor
52
53 ECM = Extracellular Matrix
54
55 ESNF = Electrospun Nanofiber
56
57 GQD = Graphene Quantum Dot
58
59 MBBS = Mass-Based Biosensor
60
MPS = Mononuclear Phagocytes System
MWCNT = Multiwall Carbon Nanotube
NF = Nanofiber

OBS = Optical Biosensor

QD = Quantum Dot

7. REFERENCES

- (1) W.H.O. *Monitoring Health for the Sustainable Development Goals: World Health Statistics 2018*; 2018.
- (2) Cancer Research UK. Cancer mortality statistics
<https://www.cancerresearchuk.org/health-professional/cancer-statistics/mortality>
(accessed Aug 19, 2018).
- (3) Vasudev, N. S.; Reynolds, A. R. Anti-Angiogenic Therapy for Cancer: Current Progress, Unresolved Questions and Future Directions. *Angiogenesis* **2014**, *17* (3), 471–494. <https://doi.org/10.1007/s10456-014-9420-y>.
- (4) Begg, A. C.; Stewart, F. A.; Vens, C. Strategies to Improve Radiotherapy with Targeted Drugs. *Nat. Rev. Cancer* **2011**, *11* (4), 239–253.
<https://doi.org/10.1038/nrc3007>.
- (5) Zong, S.; Wang, X.; Yang, Y.; Wu, W.; Li, H.; Ma, Y.; Lin, W.; Sun, T.; Huang, Y.; Xie, Z.; et al. The Use of Cisplatin-Loaded Mucoadhesive Nanofibers for Local Chemotherapy of Cervical Cancers in Mice. *Eur. J. Pharm. Biopharm.* **2015**, *93*, 127–135. <https://doi.org/10.1016/j.ejpb.2015.03.029>.
- (6) Aberoumandi, S. M.; Mohammadhosseini, M.; Abasi, E.; Saghati, S.; Nikzamir, N.; Akbarzadeh, A.; Panahi, Y.; Davaran, S. An Update on Applications of Nanostructured Drug Delivery Systems in Cancer Therapy: A Review. *Artif. Cells, Nanomedicine Biotechnol.* **2017**, *45* (6), 1058–1068.
<https://doi.org/10.1080/21691401.2016.1228658>.
- (7) Zhang, Q.; Li, Y.; Lin, Z. Y. (William); Wong, K. K. Y.; Lin, M.; Yildirim, L.;

- 1
2
3 Zhao, X. Electrospun Polymeric Micro/Nanofibrous Scaffolds for Long-Term Drug
4 Release and Their Biomedical Applications. *Drug Discov. Today* **2017**, *22* (9), 1351–
5 1366. <https://doi.org/10.1016/j.drudis.2017.05.007>.
6
7
8
9
10
11 (8) Liu, J.; Huang, Y.; Kumar, A.; Tan, A.; Jin, S.; Mozhi, A.; Liang, X. J. PH-Sensitive
12 Nano-Systems for Drug Delivery in Cancer Therapy. *Biotechnol. Adv.* **2014**, *32* (4),
13 693–710. <https://doi.org/10.1016/j.biotechadv.2013.11.009>.
14
15
16
17 (9) Goldberg, M.; Langer, R.; Jia, X. Nanostructured Materials for Applications in Drug
18 Delivery and Tissue Engineering. *J. Biomater. Sci. Polym. Ed.* **2007**, *18* (3), 241–268.
19
20 <https://doi.org/10.1163/156856207779996931>.
21
22
23
24 (10) Thakor, A. S.; Gambhir, S. S. Nanooncology: The Future of Cancer Diagnosis and
25 Therapy. *CA. Cancer J. Clin.* **2013**, *63* (6), 395–418.
26
27 <https://doi.org/10.3322/caac.21199>.
28
29
30
31 (11) Sapountzi, E.; Braiek, M.; Chateaux, J. F.; Jaffrezic-Renault, N.; Lagarde, F. Recent
32 Advances in Electrospun Nanofiber Interfaces for Biosensing Devices. *Sensors*
33 *(Switzerland)* **2017**, *17* (8), 1–29. <https://doi.org/10.3390/s17081887>.
34
35
36
37 (12) Bohunicky, B.; Mousa, S. A. Biosensors: The New Wave in Cancer Diagnosis.
38 *Nanotechnol. Sci. Appl.* **2011**, *4* (1), 1–10. <https://doi.org/10.2147/NSA.S13465>.
39
40
41
42 (13) Andre, R. S.; Sanfelice, R. C.; Pavinatto, A.; Mattoso, L. H. C.; Correa, D. S. Hybrid
43 Nanomaterials Designed for Volatile Organic Compounds Sensors: A Review. *Mater.*
44 *Des.* **2018**, *156*, 154–166. <https://doi.org/10.1016/j.matdes.2018.06.041>.
45
46
47
48 (14) Huang, L.; Wang, Z.; Zhu, X.; Chi, L. Electrical Gas Sensors Based on Structured
49 Organic Ultra-Thin Films and Nanocrystals on Solid State Substrates. *Nanoscale*
50 *Horizons* **2016**, *1* (5), 383–393. <https://doi.org/10.1039/c6nh00040a>.
51
52
53
54 (15) Chen, S.; Boda, S. K.; Batra, S. K.; Li, X.; Xie, J. Emerging Roles of Electrospun
55
56
57
58
59
60

- 1
2
3 Nanofibers in Cancer Research. *Adv. Healthc. Mater.* **2018**, *7* (6), 1–20.
4
5 <https://doi.org/10.1002/adhm.201701024>.
6
7
8 (16) Zhang, M.; Zhao, X.; Zhang, G.; Wei, G.; Su, Z. Electrospinning Design of Functional
9 Nanostructures for Biosensor Applications. *J. Mater. Chem. B* **2017**, *5* (9), 1699–1711.
10
11 <https://doi.org/10.1039/C6TB03121H>.
12
13
14
15 (17) Allen, T. M.; Cullis, P. R. Drug Delivery Systems: Entering the Mainstream. *Science*
16 (*80-*). **2004**, *303* (5665), 1818–1822. <https://doi.org/10.1126/science.1095833>.
17
18
19
20 (18) Huang, C.; Soenen, S. J.; Rejman, J.; Lucas, B.; Braeckmans, K.; Demeester, J.;
21 Smedt, S. C. De. Stimuli-Responsive Electrospun Fibers and Their Applications.
22 *Chem. Soc. Rev.* **2011**, *40*, 2417–2434. <https://doi.org/10.1039/c0cs00181c>.
23
24
25
26
27 (19) Chen, Z.; Chen, Z.; Zhang, A.; Hu, J.; Wang, X.; Yang, Z. Electrospun Nanofibers for
28 Cancer Diagnosis and Therapy. *Biomater. Sci.* **2016**, *4* (6), 922–932.
29
30
31 <https://doi.org/10.1039/C6BM00070C>.
32
33
34
35 (20) Nam, S.; Lee, S. Y.; Cho, H. J. Phloretin-Loaded Fast Dissolving Nanofibers for the
36 Locoregional Therapy of Oral Squamous Cell Carcinoma. *J. Colloid Interface Sci.*
37 **2017**, *508*, 112–120. <https://doi.org/10.1016/j.jcis.2017.08.030>.
38
39
40
41
42 (21) Radacsi, N.; Giapis, K. P.; Ovari, G.; Szabó-Révész, P.; Ambrus, R. Electrospun
43 Nanofiber-Based Niflumic Acid Capsules with Superior Physicochemical Properties.
44 *J. Pharm. Biomed. Anal.* **2019**, *166*, 371–378.
45
46
47 <https://doi.org/10.1016/j.jpba.2019.01.037>.
48
49
50
51 (22) Sharma, A.; Gupta, A.; Rath, G.; Goyal, A.; Mathur, R. B.; Dhakate, S. R. Electrospun
52 Composite Nanofiber-Based Transmucosal Patch for Anti-Diabetic Drug Delivery. *J.*
53 *Mater. Chem. B* **2013**, *1* (27), 3410–3418. <https://doi.org/10.1039/c3tb20487a>.
54
55
56
57
58 (23) Prausnitz, M. R.; Langer, R. Transdermal Drug Delivery. *TL - 26. Nat. Biotechnol.*
59
60

- 1
2
3 **2008**. <https://doi.org/10.1038/nbt.1504>.
- 4
5
6 (24) Burugapalli, K.; Wijesuriya, S.; Wang, N.; Song, W. Biomimetic Electrospun Coatings
7
8 Increase the in Vivo Sensitivity of Implantable Glucose Biosensors. *J. Biomed. Mater.*
9
10 *Res. - Part A* **2018**, *106* (4), 1072–1081. <https://doi.org/10.1002/jbm.a.36308>.
- 11
12
13 (25) Greiner, A.; Wendorff, J. H. Electrospinning: A Fascinating Method for the
14
15 Preparation of Ultrathin Fibers. *Angewandte Chemie - International Edition*. 2007, pp
16
17 5670–5703. <https://doi.org/10.1002/anie.200604646>.
- 18
19
20 (26) Long, Y. Z.; Li, M. M.; Gu, C.; Wan, M.; Duvail, J. L.; Liu, Z.; Fan, Z. Recent
21
22 Advances in Synthesis, Physical Properties and Applications of Conducting Polymer
23
24 Nanotubes and Nanofibers. *Prog. Polym. Sci.* **2011**, *36* (10), 1415–1442.
25
26 <https://doi.org/10.1016/j.progpolymsci.2011.04.001>.
- 27
28
29 (27) Davis, F. J. *Electrospinning Principles*; 2015.
- 30
31
32 (28) Khalf, A.; Madihally, S. V. Recent Advances in Multiaxial Electrospinning for Drug
33
34 Delivery. *Eur. J. Pharm. Biopharm.* **2017**, *112*, 1–17.
35
36 <https://doi.org/10.1016/j.ejpb.2016.11.010>.
- 37
38
39 (29) Textile Engineering - High Performance and Specialty Fibres. IIT Delhi.
40
41 <https://nptel.ac.in/courses/116102006/20> (accessed Jul 25, 2019).
- 42
43
44 (30) Saadati, A.; Hassanpour, S.; Guardia, M. de la; Mosafer, J.; Hashemzaei, M.;
45
46 Mokhtarzadeh, A.; Baradaran, B. Recent Advances on Application of Peptide Nucleic
47
48 Acids as a Bioreceptor in Biosensors Development. *TrAC - Trends Anal. Chem.* **2019**,
49
50 *114*, 56–68. <https://doi.org/10.1016/j.trac.2019.02.030>.
- 51
52
53 (31) Canh, T. M. Construction of Biosensors. *Biosensors* **1993**, 22–44.
54
55 https://doi.org/10.1007/978-0-585-37623-3_3.
- 56
57
58 (32) Pirzada, T.; Arvidson, S. A.; Saquing, C. D.; Shah, S. S.; Khan, S. A. Hybrid Silica-
59
60

- 1
2
3 PVA Nanofibers via Sol-Gel Electrospinning. *Langmuir* **2012**, 28 (13), 5834–5844.
4
5 <https://doi.org/10.1021/la300049j>.
6
7
8 (33) Kalra, V.; Lee, J. H.; Park, J. H.; Marquez, M.; Joo, Y. L. Confined Assembly of
9
10 Asymmetric Block-Copolymer Nanofibers via Multiaxial Jet Electrospinning. *Small*
11
12 **2009**, 5 (20), 2323–2332. <https://doi.org/10.1002/sml.200900157>.
13
14
15 (34) Li, P.; Zhang, M.; Liu, X.; Su, Z.; Wei, G. Electrostatic Assembly of Platinum
16
17 Nanoparticles along Electrospun Polymeric Nanofibers for High Performance
18
19 Electrochemical Sensors. *Nanomaterials* **2017**, 7 (9), 236.
20
21 <https://doi.org/10.3390/nano7090236>.
22
23
24 (35) Huang, Y.; Miao, Y. E.; Ji, S.; Tjiu, W. W.; Liu, T. Electrospun Carbon Nanofibers
25
26 Decorated with Ag-Pt Bimetallic Nanoparticles for Selective Detection of Dopamine.
27
28 *ACS Appl. Mater. Interfaces* **2014**, 6 (15), 12449–12456.
29
30 <https://doi.org/10.1021/am502344p>.
31
32
33 (36) Radacsi, N.; Campos, F. D.; Chisholm, C. R. I.; Giapis, K. P. Spontaneous Formation
34
35 of Nanoparticles on Electrospun Nanofibres. *Nat. Commun.* **2018**, 9 (1), 3–10.
36
37 <https://doi.org/10.1038/s41467-018-07243-5>.
38
39
40 (37) Elahi, M. F.; Lu, W. Core-Shell Fibers for Biomedical Applications-A Review. *J.*
41
42 *Bioeng. Biomed. Sci.* **2013**, 03 (01), 1–14. <https://doi.org/10.4172/2155-9538.1000121>.
43
44
45 (38) Mondal, K.; Ali, M. A.; Srivastava, S.; Malhotra, B. D.; Sharma, A. Electrospun
46
47 Functional Micro/Nanochannels Embedded in Porous Carbon Electrodes for
48
49 Microfluidic Biosensing. *Sensors Actuators, B Chem.* **2016**, 229, 82–91.
50
51 <https://doi.org/10.1016/j.snb.2015.12.108>.
52
53
54 (39) Shilpa, S.; Basavaraja, B. M.; Majumder, S. B.; Sharma, A. Electrospun Hollow
55
56 Glassy Carbon–Reduced Graphene Oxide Nanofibers with Encapsulated ZnO
57
58
59
60

- 1
2
3 Nanoparticles: A Free Standing Anode for Li-Ion Batteries. *J. Mater. Chem. A* **2015**, *3*
4 (10), 5344–5351. <https://doi.org/10.1039/C4TA07220K>.
5
6
7
8 (40) Zhao, Y.; Cao, X.; Jiang, L. Bio-Mimic Multichannel Microtubes by a Facile Method.
9
10 *J. Am. Chem. Soc.* **2007**, *129* (4), 764–765. <https://doi.org/10.1021/ja068165g>.
11
12
13 (41) Wang, C.; Yan, K. W.; Lin, Y. D.; Hsieh, P. C. H. Biodegradable Core/Shell Fibers by
14
15 Coaxial Electrospinning: Processing, Fiber Characterization, and Its Application in
16
17 Sustained Drug Release. *Macromolecules* **2010**, *43* (15), 6389–6397.
18
19
20 <https://doi.org/10.1021/ma100423x>.
21
22
23 (42) Arvidson, S. A.; Wong, K. C.; Gorga, R. E.; Khan, S. A. Structure, Molecular
24
25 Orientation, and Resultant Mechanical Properties in Core/ Sheath Poly(Lactic
26
27 Acid)/Polypropylene Composites. *Polymer (Guildf)*. **2012**, *53* (3), 791–800.
28
29
30 <https://doi.org/10.1016/j.polymer.2011.12.042>.
31
32
33 (43) Xue, J.; Wu, T.; Dai, Y.; Xia, Y. Electrospinning and Electrospun Nanofibers:
34
35 Methods, Materials, and Applications. *Chem. Rev.* **2019**, *119* (8), 5298–5415.
36
37
38 <https://doi.org/10.1021/acs.chemrev.8b00593>.
39
40
41 (44) Sun, Z.; Zussman, E.; Yarin, A. L.; Wendorff, J. H.; Greiner, A. Compound Core-Shell
42
43 Polymer Nanofibers by Co-Electrospinning. *Adv. Mater.* **2003**, *15* (22), 1929–1932.
44
45
46 <https://doi.org/10.1002/adma.200305136>.
47
48
49 (45) Rahmani, S.; Arefazar, A.; Latifi, M. PMMA / PS Coaxial Electrospinning : Core –
50
51 Shell Fiber Morphology as a Function of Material Parameters. *Mater. Res. Express*
52
53 **2017**, *035304*, 1–8.
54
55
56 (46) Díaz, J. E.; Barrero, A.; Márquez, M.; Loscertales, I. G. Controlled Encapsulation of
57
58 Hydrophobic Liquids in Hydrophilic Polymer Nanofibers by Co-Electrospinning. *Adv.*
59
60 *Funct. Mater.* **2006**, *16* (16), 2110–2116. <https://doi.org/10.1002/adfm.200600204>.

- 1
2
3
4
5
6
7
8
9
10
11
12
13
14
15
16
17
18
19
20
21
22
23
24
25
26
27
28
29
30
31
32
33
34
35
36
37
38
39
40
41
42
43
44
45
46
47
48
49
50
51
52
53
54
55
56
57
58
59
60
- (47) Loscertales, I. G.; Barrero, A.; Márquez, M.; Spretz, R.; Velarde-Ortiz, R.; Larsen, G. Electrically Forced Coaxial Nanojets for One-Step Hollow Nanofiber Design. *J. Am. Chem. Soc.* **2004**, *126* (17), 5376–5377. <https://doi.org/10.1021/ja049443j>.
- (48) Li, D.; Xia, Y. Direct Fabrication of Composite and Ceramic Hollow Nanofibers by Electrospinning. *Nano Lett.* **2004**, *4* (5), 933–938. <https://doi.org/10.1021/nl049590f>.
- (49) Moghe, A. K.; Gupta, B. S. Co-Axial Electrospinning for Nanofiber Structures: Preparation and Applications. *Polym. Rev.* **2008**, *48* (2), 353–377. <https://doi.org/10.1080/15583720802022257>.
- (50) Sill, T. J.; von Recum, H. A. Electrospinning: Applications in Drug Delivery and Tissue Engineering. *Biomaterials* **2008**, *29* (13), 1989–2006. <https://doi.org/10.1016/j.biomaterials.2008.01.011>.
- (51) Hong, J. K.; Madhally, S. V. Next Generation of Electrospayed Fibers for Tissue Regeneration. *Tissue Eng. Part B Rev.* **2011**, *17* (2), 125–142. <https://doi.org/10.1089/ten.teb.2010.0552>.
- (52) Ruoslahti, E.; Engvall, E. Integrins and Vascular Extracellular Matrix Assembly. *J. Clin. Invest.* **1997**, *99* (6), 1149–1152. <https://doi.org/10.1172/JCI119269>.
- (53) Lawrence, B. J.; Madhally, S. V. Cell Colonization in Degradable 3D Porous Matrices. *Cell Adh. Migr.* **2008**, *2* (1), 9–16. <https://doi.org/10.4161/cam.2.1.5884>.
- (54) Brigger, I.; Dubernet, C.; Couvreur, P. Nanoparticles in Cancer Therapy and Diagnosis. *Adv. Drug Deliv. Rev.* **2002**, *54* (5), 631–651. [https://doi.org/10.1016/S0169-409X\(02\)00044-3](https://doi.org/10.1016/S0169-409X(02)00044-3).
- (55) Byrne, J. D.; Betancourt, T.; Brannon-Peppas, L. Active Targeting Schemes for Nanoparticle Systems in Cancer Therapeutics. *Adv. Drug Deliv. Rev.* **2008**, *60* (15), 1615–1626. <https://doi.org/10.1016/j.addr.2008.08.005>.

- 1
2
3 (56) Pasinszki, T.; Krebsz, M.; Tung, T. T.; Losic, D. Carbon Nanomaterial Based
4 Biosensors for Non-Invasive Detection of Cancer and Disease Biomarkers for Clinical
5 Diagnosis. *Sensors* **2017**, *17* (8), 1–32. <https://doi.org/10.3390/s17081919>.
6
7
8
9
10 (57) Liang, D.; Luu, Y. K.; Kim, K.; Hsiao, B. S.; Hadjiargyrou, M.; Chu, B. In Vitro Non-
11 Viral Gene Delivery with Nanofibrous Scaffolds. *Nucleic Acids Res.* **2005**, *33* (19), 1–
12 10. <https://doi.org/10.1093/nar/gni171>.
13
14
15
16
17 (58) Luong-Van, E.; Grøndahl, L.; Chua, K. N.; Leong, K. W.; Nurcombe, V.; Cool, S. M.
18 Controlled Release of Heparin from Poly(ϵ -Caprolactone) Electrospun Fibers.
19 *Biomaterials* **2006**, *27* (9), 2042–2050.
20 <https://doi.org/10.1016/j.biomaterials.2005.10.028>.
21
22
23
24
25
26
27 (59) Wang, H.; Feng, Y.; Zhao, H.; Lu, J.; Guo, J.; Behl, M.; Lendlein, A. Controlled
28 Heparin Release from Electrospun Gelatin Fibers. *J. Control. Release* **2011**, *152 Suppl*
29 (2011), e28-9. <https://doi.org/10.1016/j.jconrel.2011.08.102>.
30
31
32
33
34 (60) Keusgen, M. Biosensors: New Approaches in Drug Discovery. *Naturwissenschaften*
35 **2002**, *89* (10), 433–444. <https://doi.org/10.1007/s00114-002-0358-3>.
36
37
38
39 (61) Wagner, V.; Dullaart, A.; Bock, A. K.; Zweck, A. The Emerging Nanomedicine
40 Landscape. *Nat. Biotechnol.* **2006**, *24* (10), 1211–1217.
41 <https://doi.org/10.1038/nbt1006-1211>.
42
43
44
45
46 (62) Bobo, D.; Robinson, K. J.; Islam, J.; Thurecht, K. J.; Corrie, S. R. Nanoparticle-Based
47 Medicines: A Review of FDA-Approved Materials and Clinical Trials to Date. *Pharm.*
48 *Res.* **2016**, *33* (10), 2373–2387. <https://doi.org/10.1007/s11095-016-1958-5>.
49
50
51
52
53 (63) Chambers, J. P.; Arulanandam, B. P.; Matta, L. L.; Weis, A.; Valdes, J. J. Biosensor
54 Recognition Elements. *Curr. Issues Mol. Biol.* **2002**, 1–12.
55
56
57
58 (64) Anu Bhushani, J.; Anandharamakrishnan, C. Electrospinning and Electrospraying
59
60

- 1
2
3 Techniques: Potential Food Based Applications. *Trends Food Sci. Technol.* **2014**, *38*
4 (1), 21–33. <https://doi.org/10.1016/j.tifs.2014.03.004>.
5
6
7
8 (65) Mehrotra, P. Biosensors and Their Applications - A Review. *J. Oral Biol. Craniofacial*
9 *Res.* **2016**, *6* (2), 153–159. <https://doi.org/10.1016/j.jobcr.2015.12.002>.
10
11
12
13 (66) Gringoz, A.; Glandut, N.; Valette, S. Electrochemical Hydrogen Storage in TiC_{0.6},
14 Not in TiC_{0.9}. *Electrochem. commun.* **2009**, *11* (10), 2044–2047.
15
16
17 <https://doi.org/10.1016/j.elecom.2009.08.049>.
18
19
20 (67) Zhang, B.; Cui, T. An Ultrasensitive and Low-Cost Graphene Sensor Based on Layer-
21 by-Layer Nano Self-Assembly. *Appl. Phys. Lett.* **2011**, *98* (7).
22
23 <https://doi.org/10.1063/1.3557504>.
24
25
26
27 (68) Bonifert, G.; Folkes, L.; Gmeiner, C.; Dachs, G.; Spadiut, O. Recombinant
28 Horseradish Peroxidase Variants for Targeted Cancer Treatment. *Cancer Med.* **2016**, *5*
29 (6), 1194–1203. <https://doi.org/10.1002/cam4.668>.
30
31
32
33 (69) Liang, S.-L.; Chan, D. W. Enzymes and Related Proteins as Cancer Biomarkers: A
34 Proteomic Approach. *Clin Chim Acta* **2013**, *18* (9), 1199–1216.
35
36
37 <https://doi.org/10.1016/j.micinf.2011.07.011>.
38
39
40
41 (70) Yarden, Y. The EGFR Family and Its Ligands in Human Cancer: Signaling
42 Mechanisms and Therapeutic Opportunities. *J. Parasitol.* **1973**, *59* (5), 753–758.
43
44
45 <https://doi.org/10.2307/3278399>.
46
47
48
49 (71) Ralla, B.; Stephan, C.; Meller, S.; Dietrich, D.; Kristiansen, G.; Jung, K. Nucleic Acid-
50 Based Biomarkers in Body Fluids of Patients with Urologic Malignancies. *Crit. Rev.*
51 *Clin. Lab. Sci.* **2014**, *51* (4), 200–231. <https://doi.org/10.3109/10408363.2014.914888>.
52
53
54
55 (72) Schwarzenbach, H. Circulating Nucleic Acids as Biomarkers in Breast Cancer. *Breast*
56 *Cancer Res.* **2013**, *15* (5), 211. <https://doi.org/10.1186/bcr3446>.
57
58
59
60

- 1
2
3 (73) Liebana, S.; Drago, G. A. Bioconjugation and Stabilisation of Biomolecules in
4 Biosensors. *Essays Biochem.* **2016**, *60* (1), 59–68.
5
6 <https://doi.org/10.1042/EBC20150007>.
7
8
9
10 (74) Bhardwaj, T. A Review on Immobilization Techniques of Biosensors. *Int. J. Eng. Res.*
11 *Technol.* **2014**, *3* (5), 294–298.
12
13
14 (75) Hermanson, G. T. Introduction to Bioconjugation. In *Bioconjugate Techniques*;
15 Hermanson, G. T., Ed.; Elsevier, 2013; pp 1–125. [https://doi.org/10.1016/B978-0-12-](https://doi.org/10.1016/B978-0-12-382239-0.00001-7)
16 [382239-0.00001-7](https://doi.org/10.1016/B978-0-12-382239-0.00001-7).
17
18
19
20 (76) Rogers, K. R. Principles of Affinity-Based Biosensors. *Mol. Biotechnol.* **2000**, *14* (2),
21 109–130. <https://doi.org/10.1385/MB:14:2:109>.
22
23
24 (77) Putzbach, W.; Ronkainen, N. J. Immobilization Techniques in the Fabrication of
25 Nanomaterial-Based Electrochemical Biosensors: A Review. *Sensors (Switzerland)*
26 **2013**, *13* (4), 4811–4840. <https://doi.org/10.3390/s130404811>.
27
28
29 (78) Brena, B. M.; Batista-Viera, F. Immobilization of Enzymes: A Literature Survey. In
30 *Immobilization of Enzyme and Cells*; Guisan, J., Ed.; Humana Press, 2006; pp 15–30.
31 https://doi.org/10.1007/978-1-62703-550-7_2.
32
33
34 (79) Grieshaber, D.; MacKenzie, R.; Vörös, J.; Reimhult, E. Electrochemical Biosensors -
35 Sensor Principles and Architectures. *Sensors* **2008**, *8* (3), 1400–1458.
36 <https://doi.org/10.3390/s8031400>.
37
38
39 (80) Clark, L. C.; Lyons, C. Electrode Systems for Continuous Monitoring in
40 Cardiovascular Surgery. *Ann. N. Y. Acad. Sci.* **2006**, *102* (1), 29–45.
41 <https://doi.org/10.1111/j.1749-6632.1962.tb13623.x>.
42
43
44 (81) Wei, Y.; Li, X.; Sun, X.; Ma, H.; Zhang, Y.; Wei, Q. Dual-Responsive
45 Electrochemical Immunosensor for Prostate Specific Antigen Detection Based on Au-
46
47
48
49
50
51
52
53
54
55
56
57
58
59
60

- 1
2
3 CoS/Graphene and CeO₂/Ionic Liquids Doped with Carboxymethyl Chitosan
4
5 Complex. *Biosens. Bioelectron.* **2017**, *94* (January), 141–147.
6
7 <https://doi.org/10.1016/j.bios.2017.03.001>.
8
9
10 (82) MEHRVAR, M.; ABDI, M. Recent Developments, Characteristics, and Potential
11 Applications of Electrochemical Biosensors. *Anal. Sci.* **2004**, *20* (8), 1113–1126.
12
13 <https://doi.org/10.2116/analsci.20.1113>.
14
15
16
17 (83) Marcus, R. A.; Sutin, N. Electron Transfers in Chemistry and Biology. *BBA Rev.*
18 *Bioenerg.* **1985**, *811* (3), 265–322. [https://doi.org/10.1016/0304-4173\(85\)90014-X](https://doi.org/10.1016/0304-4173(85)90014-X).
19
20
21
22 (84) Yan, L.; Chen, X. *Nanomaterials for Drug Delivery*, Second Edi.; Elsevier Ltd, 2017.
23
24 https://doi.org/10.1007/978-3-319-63633-7_5.
25
26
27 (85) Tîlmaciu, C.-M.; Morris, M. C. Carbon Nanotube Biosensors. *Front. Chem.* **2015**, *3*
28 (October), 1–21. <https://doi.org/10.3389/fchem.2015.00059>.
29
30
31
32 (86) Li, Y.; Zhang, M.; Zhang, X.; Xie, G.; Su, Z.; Wei, G. Nanoporous Carbon Nanofibers
33 Decorated with Platinum Nanoparticles for Non-Enzymatic Electrochemical Sensing
34 of H₂O₂. *Nanomaterials* **2015**, *5* (4), 1891–1905.
35
36 <https://doi.org/10.3390/nano5041891>.
37
38
39
40 (87) Yu, J.; Zhang, X.; Hao, X.; Zhang, X.; Zhou, M.; Lee, C. S.; Chen, X. Near-Infrared
41 Fluorescence Imaging Using Organic Dye Nanoparticles. *Biomaterials* **2014**, *35* (10),
42
43 3356–3364. <https://doi.org/10.1016/j.biomaterials.2014.01.004>.
44
45
46
47 (88) Lan, M.; Zhang, J.; Zhu, X.; Wang, P.; Chen, X.; Lee, C. S.; Zhang, W. Highly Stable
48 Organic Fluorescent Nanorods for Living-Cell Imaging. *Nano Res.* **2015**, *8* (7), 2380–
49
50 2389. <https://doi.org/10.1007/s12274-015-0748-4>.
51
52
53
54 (89) Yu, J.; Diao, X.; Zhang, X.; Chen, X.; Hao, X.; Li, W.; Zhang, X.; Lee, C. S. Water-
55
56 Dispersible, Ph-Stable and Highly-Luminescent Organic Dye Nanoparticles with
57
58
59
60

- 1
2
3 Amplified Emissions for in Vitro and in Vivo Bioimaging. *Small* **2014**, *10* (6), 1125–
4 1132. <https://doi.org/10.1002/sml.201302230>.
5
6
7
8 (90) Xu, R.; Huang, L.; Wei, W.; Chen, X.; Zhang, X.; Zhang, X. Real-Time Imaging and
9 Tracking of Ultrastable Organic Dye Nanoparticles in Living Cells. *Biomaterials* **2016**,
10 *93*, 38–47. <https://doi.org/10.1016/j.biomaterials.2016.03.045>.
11
12
13
14
15 (91) Chen, X.; Zhang, W. Diamond Nanostructures for Drug Delivery, Bioimaging, and
16 Biosensing. *Chem. Soc. Rev.* **2017**, *46* (3), 734–760.
17
18
19 <https://doi.org/10.1039/c6cs00109b>.
20
21
22
23 (92) Devadoss, A.; Han, H.; Song, T.; Kim, Y.-P.; Paik, U. Gold Nanoparticle-Composite
24 Nanofibers for Enzymatic Electrochemical Sensing of Hydrogen Peroxide. *Analyst*
25 **2013**, *138* (17), 5025. <https://doi.org/10.1039/c3an00317e>.
26
27
28
29
30 (93) Crespy, D.; Friedemann, K.; Popa, A. M. Colloid-Electrospinning: Fabrication of
31 Multicompartment Nanofibers by the Electrospinning of Organic or/and Inorganic
32 Dispersions and Emulsions. *Macromol. Rapid Commun.* **2012**, *33* (23), 1978–1995.
33
34
35
36 <https://doi.org/10.1002/marc.201200549>.
37
38
39
40 (94) Li, Z.; Wang, C. Effects of Working Parameters on Electrospinning. In *One*
41 *Dimensional Nanostructures*; 2013; pp 15–29. [https://doi.org/10.1007/978-3-642-](https://doi.org/10.1007/978-3-642-36427-3)
42 [36427-3](https://doi.org/10.1007/978-3-642-36427-3).
43
44
45
46 (95) Brown, T. D.; Dalton, P. D.; Hutmacher, D. W. Melt Electrospinning Today: An
47 Opportune Time for an Emerging Polymer Process. *Prog. Polym. Sci.* **2015**, *56*, 116–
48 166. <https://doi.org/10.1016/j.progpolymsci.2016.01.001>.
49
50
51
52
53
54 (96) Ali, M. A.; Mondal, K.; Singh, C.; Dhar Malhotra, B.; Sharma, A. Anti-Epidermal
55 Growth Factor Receptor Conjugated Mesoporous Zinc Oxide Nanofibers for Breast
56 Cancer Diagnostics. *Nanoscale* **2015**, *7* (16), 7234–7245.
57
58
59
60

- 1
2
3 <https://doi.org/10.1039/C5NR00194C>.
- 4
5
6 (97) Baj-Rossi, C.; de Micheli, G.; Carrara, S. Electrochemical Detection of Anti-Breast-
7
8 Cancer Agents in Human Serum by Cytochrome P450-Coated Carbon Nanotubes.
9
10 *Sensors (Switzerland)* **2012**, *12* (5), 6520–6537. <https://doi.org/10.3390/s120506520>.
- 11
12
13 (98) Campuzano, S.; Yáñez-Sedeño, P.; Pingarrón, J. Diagnostics Strategies with
14
15 Electrochemical Affinity Biosensors Using Carbon Nanomaterials as Electrode
16
17 Modifiers. *Diagnostics* **2016**, *7* (1), 2. <https://doi.org/10.3390/diagnostics7010002>.
- 18
19
20 (99) Tripathy, S.; Krishna Vanjari, S. R.; Singh, V.; Swaminathan, S.; Singh, S. G.
21
22 Electrospun Manganese (III) Oxide Nanofiber Based Electrochemical DNA-
23
24 Nanobiosensor for Zeptomolar Detection of Dengue Consensus Primer. *Biosens.*
25
26 *Bioelectron.* **2017**, *90* (December 2016), 372–387.
27
28 <https://doi.org/10.1016/j.bios.2016.12.008>.
- 29
30
31 (100) Mittal, V. Preface. In *In-situ Synthesis of Polymer Nanocomposites*; 2012; pp XIII–
32
33 XIV.
- 34
35
36 (101) Liu, Z.; Zhou, C.; Zheng, B.; Qian, L.; Mo, Y.; Luo, F.; Shi, Y.; Choi, M. M. F.; Xiao,
37
38 D. In Situ Synthesis of Gold Nanoparticles on Porous Polyacrylonitrile Nanofibers for
39
40 Sensing Applications. *Analyst* **2011**, *136* (21), 4545.
41
42 <https://doi.org/10.1039/c1an15330g>.
- 43
44
45 (102) Zhang, P.; Zhao, X.; Zhang, X.; Lai, Y.; Wang, X.; Li, J.; Wei, G.; Su, Z. Electrospun
46
47 Doping of Carbon Nanotubes and Platinum Nanoparticles into the β -Phase
48
49 Polyvinylidene Difluoride Nanofibrous Membrane for Biosensor and Catalysis
50
51 Applications. *ACS Appl. Mater. Interfaces* **2014**, *6* (10), 7563–7571.
52
53 <https://doi.org/10.1021/am500908v>.
- 54
55
56 (103) Gupta, K. K.; Mishra, P. K.; Srivastava, P.; Gangwar, M.; Nath, G.; Maiti, P.
57
58
59
60

- 1
2
3 Hydrothermal in Situ Preparation of TiO₂ particles onto Poly(Lactic Acid) Electrospun
4 Nanofibres. *Appl. Surf. Sci.* **2013**, *264*, 375–382.
5
6 <https://doi.org/10.1016/j.apsusc.2012.10.029>.
7
8
9
10 (104) Mondal, K.; Ali, M. A.; Agrawal, V. V.; Malhotra, B. D.; Sharma, A. Highly Sensitive
11 Biofunctionalized Mesoporous Electrospun TiO₂ nanofiber Based Interface for
12 Biosensing. *ACS Appl. Mater. Interfaces* **2014**, *6* (4), 2516–2527.
13
14 <https://doi.org/10.1021/am404931f>.
15
16
17
18 (105) Mondal, K.; Bhattacharyya, S.; Sharma, A. Photocatalytic Degradation of Naphthalene
19 by Electrospun Mesoporous Carbon-Doped Anatase TiO₂ nanofiber Mats. *Ind. Eng.*
20 *Chem. Res.* **2014**, *53* (49), 18900–18909. <https://doi.org/10.1021/ie5025744>.
21
22
23
24 (106) Fong, W. K.; Negrini, R.; Vallooran, J. J.; Mezzenga, R.; Boyd, B. J. Responsive Self-
25 Assembled Nanostructured Lipid Systems for Drug Delivery and Diagnostics. *J.*
26 *Colloid Interface Sci.* **2016**, *484*, 320–339. <https://doi.org/10.1016/j.jcis.2016.08.077>.
27
28
29
30 (107) Soikkeli, M.; Kurppa, K.; Kainlauri, M.; Arpiainen, S.; Paananen, A.; Gunnarsson, D.;
31 Joensuu, J. J.; Laaksonen, P.; Prunnila, M.; Linder, M. B.; et al. Graphene Biosensor
32 Programming with Genetically Engineered Fusion Protein Monolayers. *ACS Appl.*
33 *Mater. Interfaces* **2016**, *8* (12), 8257–8264. <https://doi.org/10.1021/acsami.6b00123>.
34
35
36
37 (108) Li, L.; Li, W.; Ma, C.; Yang, H.; Ge, S.; Yu, J. Paper-Based
38 Electrochemiluminescence Immunodevice for Carcinoembryonic Antigen Using
39 Nanoporous Gold-Chitosan Hybrids and Graphene Quantum Dots Functionalized
40 Au@Pt. *Sensors Actuators, B Chem.* **2014**, *202*, 314–322.
41
42 <https://doi.org/10.1016/j.snb.2014.05.087>.
43
44
45
46 (109) Li, L.; Wang, X.; Liu, G.; Wang, Z.; Wang, F.; Guo, X.; Wen, Y.; Yang, H.
47
48
49
50
51
52
53
54
55
56
57
58
59
60

- Decorated Polypyrrole-Coated-Polycaprolactone-Nanofiber-Based Cloth Electrode for Electrochemical Sensor Application. *Nanotechnology* **2015**, *26* (44), 445704. <https://doi.org/10.1088/0957-4484/26/44/445704>.
- (110) Shen, J.; Yang, X.; Zhu, Y.; Kang, H.; Cao, H.; Li, C. Gold-Coated Silica-Fiber Hybrid Materials for Application in a Novel Hydrogen Peroxide Biosensor. *Biosens. Bioelectron.* **2012**, *34* (1), 132–136. <https://doi.org/10.1016/j.bios.2012.01.031>.
- (111) Cui, K.; Song, Y.; Guo, Q.; Xu, F.; Zhang, Y.; Shi, Y.; Wang, L.; Hou, H.; Li, Z. Architecture of Electrospun Carbon Nanofibers-Hydroxyapatite Composite and Its Application Act as a Platform in Biosensing. *Sensors Actuators, B Chem.* **2011**, *160* (1), 435–440. <https://doi.org/10.1016/j.snb.2011.08.005>.
- (112) Whitesides, G. M. The Origins and the Future of Microfluidics. *Nature* **2006**, *442* (7101), 368–373. <https://doi.org/10.1038/nature05058>.
- (113) Beebe, D. J.; Mensing, G. A.; Walker, G. M. Physics and Applications of Microfluidics in Biology. *Annu. Rev. Biomed. Eng.* **2002**, *4* (1), 261–286. <https://doi.org/10.1146/annurev.bioeng.4.112601.125916>.
- (114) Guarino, V.; Ambrosio, L. *Electrofluidodynamic Technologies (EFDTs) for Biomaterials and Medical Devices : Principles and Advances*; Guarino, V., Ambrosio, L., Eds.; Woodhead Publishing, 2018, 2018.
- (115) Schoch, R. B.; Cheow, L. F.; Han, J. Electrical Detection of Fast Reaction Kinetics in Nanochannels with an Induced Flow. *Nano Lett.* **2007**, *7* (12), 3895–3900. <https://doi.org/10.1021/nl0724788>.
- (116) Sackmann, E. K.; Fulton, A. L.; Beebe, D. J. The Present and Future Role of Microfluidics in Biomedical Research. *Nature* **2014**, *507* (7491), 181–189. <https://doi.org/10.1038/nature13118>.

- 1
2
3 (117) Jan, Y. J.; Chen, J. F.; Zhu, Y.; Lu, Y. T.; Chen, S. H.; Chung, H.; Smalley, M.;
4
5 Huang, Y. W.; Dong, J.; Chen, L. C.; et al. NanoVelcro Rare-Cell Assays for
6
7 Detection and Characterization of Circulating Tumor Cells. *Adv. Drug Deliv. Rev.*
8
9 **2018**, *125*, 78–93. <https://doi.org/10.1016/j.addr.2018.03.006>.
10
11
12 (118) Chen, J.-F.; Zhu, Y.; Lu, Y.-T.; Hodara, E.; Hou, S.; Agopian, V. G.; Tomlinson, J. S.;
13
14 Posadas, E. M.; Tseng, H.-R. Clinical Applications of NanoVelcro Rare-Cell Assays
15
16 for Detection and Characterization of Circulating Tumor Cells. *Theranostics* **2016**, *6*
17
18 (9), 1425–1439. <https://doi.org/10.7150/thno.15359>.
19
20
21 (119) Ji, X.; Su, Z.; Wang, P.; Ma, G.; Zhang, S. Polyelectrolyte Doped Hollow Nanofibers
22
23 for Positional Assembly of Bienzyme System for Cascade Reaction at O/W Interface.
24
25 *ACS Catal.* **2014**, *4* (12), 4548–4559. <https://doi.org/10.1021/cs501383j>.
26
27
28 (120) Tothill, I. E. Biosensors for Cancer Markers Diagnosis. *Semin. Cell Dev. Biol.* **2009**,
29
30 *20* (1), 55–62. <https://doi.org/10.1016/j.semcdb.2009.01.015>.
31
32
33 (121) Lin, J.; Yan, F.; Ju, H. Noncompetitive Enzyme Immunoassay for Carcinoembryonic
34
35 Antigen by Flow Injection Chemiluminescence. *Clin. Chim. Acta* **2004**, *341* (1–2),
36
37 109–115. <https://doi.org/10.1016/j.cccn.2003.11.014>.
38
39
40 (122) Besselink, G. A. J.; Kooyman, R. P. H.; Van Os, P. J. H. J.; Engbers, G. H. M.;
41
42 Schasfoort, R. B. M. Signal Amplification on Planar and Gel-Type Sensor Surfaces in
43
44 Surface Plasmon Resonance-Based Detection of Prostate-Specific Antigen. *Anal.*
45
46 *Biochem.* **2004**, *333* (1), 165–173. <https://doi.org/10.1016/j.ab.2004.05.009>.
47
48
49 (123) Davis, B. W.; Burriss, A. J.; Niamnont, N.; Hare, C. D.; Chen, C. Y.; Sukwattanasinitt,
50
51 M.; Cheng, Q. Dual-Mode Optical Sensing of Organic Vapors and Proteins with
52
53 Polydiacetylene (PDA)-Embedded Electrospun Nanofibers. *Langmuir* **2014**, *30* (31),
54
55 9616–9622. <https://doi.org/10.1021/la5017388>.
56
57
58
59
60

- 1
2
3 (124) Medina, V. A.; Rivera, E. S. Histamine Receptors and Cancer Pharmacology. *Br. J.*
4
5 *Pharmacol.* **2010**, *161* (4), 755–767. <https://doi.org/10.1111/j.1476->
6
7 5381.2010.00961.x.
8
9
10 (125) Siegel, R.; Miler, K.; Jemal, A. Cancer Statistics, 2017. *CA. Cancer J. Clin.* **2017**, *67*
11
12 (1), 7–30. <https://doi.org/10.3322/caac.21387>.
13
14
15 (126) Clinton Ifegwu, O.; Anyakora, C.; Torto, N. Nylon 6–Gold Nanoparticle Composite
16
17 Fibers for Colorimetric Detection of Urinary 1-Hydroxypyrene. *J. Appl. Spectrosc.*
18
19 **2015**, *82* (2), 266–271. <https://doi.org/10.1007/s10812-015-0095-y>.
20
21
22 (127) Wang, H.; Wang, D.; Peng, Z.; Tang, W.; Li, N.; Liu, F. Assembly of DNA-
23
24 Functionalized Gold Nanoparticles on Electrospun Nanofibers as a Fluorescent Sensor
25
26 for Nucleic Acids. *Chem. Commun.* **2013**, *49* (49), 5568.
27
28 <https://doi.org/10.1039/c3cc41753k>.
29
30
31 (128) Glazer, E. S.; Zhu, C.; Massey, K. L.; Thompson, C. S.; Kaluarachchi, W. D.; Hamir,
32
33 A. N.; Curley, S. A. Noninvasive Radiofrequency Field Destruction of Pancreatic
34
35 Adenocarcinoma Xenografts Treated with Targeted Gold Nanoparticles. *Clin. Cancer*
36
37 *Res.* **2010**, *16* (23), 5712–5721. <https://doi.org/10.1158/1078-0432.CCR-10-2055>.
38
39
40 (129) Lee, C.; Wood, D.; Edmondson, D.; Yao, D.; Erickson, A. E.; Tsao, C. T.; Revia, R.
41
42 A.; Kim, H.; Zhang, M. Electrospun Uniaxially-Aligned Composite Nanofibers as
43
44 Highly-Efficient Piezoelectric Material. *Ceram. Int.* **2016**, *42* (2), 2734–2740.
45
46 <https://doi.org/10.1016/j.ceramint.2015.10.170>.
47
48
49 (130) Aqeel, S. M.; Wang, Z.; Than, L.; Sreenivasulu, G.; Zeng, X. Poly(Vinylidene
50
51 Fluoride)/Poly(Acrylonitrile) – Based Superior Hydrophobic Piezoelectric Solid
52
53 Derived by Aligned Carbon Nanotubes in Electrospinning: Fabrication, Phase
54
55 Conversion and Surface Energy. *RSC Adv.* **2015**, *5* (93), 76383–76391.
56
57
58
59
60

- 1
2
3 <https://doi.org/10.1039/C5RA11584A>.
- 4
5
6 (131) Zhao, G.; Huang, B.; Zhang, J.; Wang, A.; Ren, K.; Wang, Z. L. Electrospun Poly(L-
7 Lactic Acid) Nanofibers for Nanogenerator and Diagnostic Sensor Applications.
8 *Macromol. Mater. Eng.* **2017**, *302* (5), 1–7. <https://doi.org/10.1002/mame.201600476>.
9
10
11
12
13 (132) Sencadas, V.; Ribeiro, C.; Heredia, A.; Bdikin, I. K.; Kholkin, A. L.; Lanceros-
14 Mendez, S. Local Piezoelectric Activity of Single Poly(L-Lactic Acid) (PLLA)
15 Microfibers. *Appl. Phys. A Mater. Sci. Process.* **2012**, *109* (1), 51–55.
16
17
18
19
20 <https://doi.org/10.1007/s00339-012-7095-z>.
21
22
23 (133) Sasaki, S.; Asakura, T. Helix Distortion and Crystal Structure of the α -Form of
24 Poly(L-Lactide). *Macromolecules* **2003**, *36* (22), 8385–8390.
25
26
27 <https://doi.org/10.1021/ma0348674>.
28
29
30 (134) González, E.; Frey, M. W. Synthesis, Characterization and Electrospinning of
31 Poly(Vinyl Caprolactam-Co-Hydroxymethyl Acrylamide) to Create Stimuli-
32 Responsive Nanofibers. *Polym. (United Kingdom)* **2017**, *108*, 154–162.
33
34
35
36
37 <https://doi.org/10.1016/j.polymer.2016.11.053>.
38
39
40 (135) Kong, G.; Braun, R. D.; Dewhirst, M. W. Hyperthermia Enables Tumor-Specific
41 Nanoparticle Delivery: Effect of Particle Size. *Cancer Res.* **2000**, *60* (16), 4440–4445.
42
43
44 <https://doi.org/10.1073/PNAS.72.3.937>.
45
46
47 (136) Vinogradov, S. V.; Bronich, T. K.; Kabanov, A. V. Nanosized Cationic Hydrogels for
48 Drug Delivery: Preparation, Properties and Interactions with Cells. *Adv. Drug Deliv.*
49 *Rev.* **2002**, *54* (1), 135–147. [https://doi.org/10.1016/S0169-409X\(01\)00245-9](https://doi.org/10.1016/S0169-409X(01)00245-9).
50
51
52
53
54 (137) Ogawara, K. I.; Yoshida, M.; Furumoto, K.; Takakura, Y.; Hashida, M.; Higaki, K.;
55 Kimura, T. Uptake by Hepatocytes and Biliary Excretion of Intravenously
56 Administered Polystyrene Microspheres in Rats. *J. Drug Target.* **1999**, *7* (3), 213–221.
57
58
59
60

- 1
2
3 <https://doi.org/10.3109/10611869909085504>.
- 4
5
6 (138) Mable, C. J.; Gibson, R. R.; Prevost, S.; McKenzie, B. E.; Mykhaylyk, O. O.; Armes,
7
8 S. P. Loading of Silica Nanoparticles in Block Copolymer Vesicles during
9
10 Polymerization-Induced Self-Assembly: Encapsulation Efficiency and Thermally
11
12 Triggered Release. *J. Am. Chem. Soc.* **2015**, *137* (51), 16098–16108.
13
14 <https://doi.org/10.1021/jacs.5b10415>.
- 15
16
17 (139) Zhang, J.; Li, Y.; An, F. F.; Zhang, X.; Chen, X.; Lee, C. S. Preparation and Size
18
19 Control of Sub-100 Nm Pure Nanodrugs. *Nano Lett.* **2015**, *15* (1), 313–318.
20
21 <https://doi.org/10.1021/nl503598u>.
- 22
23
24 (140) Yan, L.; Chen, X.; Wang, Z.; Zhang, X.; Zhu, X.; Zhou, M.; Chen, W.; Huang, L.;
25
26 Roy, V. A. L.; Yu, P. K. N.; et al. Size Controllable and Surface Tunable Zeolitic
27
28 Imidazolate Framework-8-Poly(Acrylic Acid Sodium Salt) Nanocomposites for PH
29
30 Responsive Drug Release and Enhanced in Vivo Cancer Treatment. *ACS Appl. Mater.*
31
32 *Interfaces* **2017**, *9* (38), 32990–33000. <https://doi.org/10.1021/acsami.7b10064>.
- 33
34
35 (141) Sercombe, L.; Veerati, T.; Moheimani, F.; Wu, S. Y.; Sood, A. K.; Hua, S. Advances
36
37 and Challenges of Liposome Assisted Drug Delivery. *Front. Pharmacol.* **2015**, *6*
38
39 (DEC), 1–13. <https://doi.org/10.3389/fphar.2015.00286>.
- 40
41
42 (142) Ghafoor, B.; Aleem, A.; Najabat Ali, M.; Mir, M. Review of the Fabrication
43
44 Techniques and Applications of Polymeric Electrospun Nanofibers for Drug Delivery
45
46 Systems. *J. Drug Deliv. Sci. Technol.* **2018**, *48* (August), 82–87.
47
48 <https://doi.org/10.1016/j.jddst.2018.09.005>.
- 49
50
51 (143) Radacsi, N.; Giapis, K. P.; Ovari, G.; Szabó-révész, P.; Ambrus, R. Electrospun
52
53 Nanofiber-Based Niflumic Acid Capsules with Superior Physicochemical Properties.
54
55 *J. Pharm. Biomed. Anal.* **2019**, *166*, 371–378.
56
57
58
59
60

- 1
2
3 <https://doi.org/10.1016/j.jpba.2019.01.037>.
- 4
5
6 (144) Chou, S.; Carson, D.; Woodrow, K. A. Current Strategies for Sustaining Drug Release
7
8 from Electrospun Nanofibers. *J. Control. Release* **2015**, *220* (1), 584–591.
9
10 <https://doi.org/10.1016/j.jconrel.2015.09.008>.Current.
- 11
12
13 (145) Ambrus, R.; Alshweiat, A.; Csóka, I.; Ovari, G.; Esmail, A.; Radacsi, N. 3D-Printed
14
15 Electrospinning Setup for the Preparation of Loratadine Nanofibers with Enhanced
16
17 Physicochemical Properties. *Int. J. Pharm.* **2019**, 118455.
18
19 <https://doi.org/10.1016/j.ijpharm.2019.118455>.
- 20
21
22 (146) Samprasit, W.; Akkaramongkolporn, P.; Ngawhirunpat, T.; Rojanarata, T.;
23
24 Kaomongkolgit, R.; Opanasopit, P. Fast Releasing Oral Electrospun PVP/CD
25
26 Nanofiber Mats of Taste-Masked Meloxicam. *Int. J. Pharm.* **2015**.
27
28 <https://doi.org/10.1016/j.ijpharm.2015.04.044>.
- 29
30
31 (147) Wen, P.; Zong, M. H.; Hu, T. G.; Li, L.; Wu, H. Preparation and Characterization of
32
33 Electrospun Colon-Specific Delivery System for Quercetin and Its Antiproliferative
34
35 Effect on Cancer Cells. *J. Agric. Food Chem.* **2018**, *66* (44), 11550–11559.
36
37 <https://doi.org/10.1021/acs.jafc.8b02614>.
- 38
39
40 (148) Gavhane, Y. N.; Yadav, A. V. Loss of Orally Administered Drugs in GI Tract. *Saudi*
41
42 *Pharm. J.* **2012**, *20* (4), 331–344. <https://doi.org/10.1016/j.jsps.2012.03.005>.
- 43
44
45 (149) Ding, Y.; Li, W.; Zhang, F.; Liu, Z.; Zanjanzadeh Ezazi, N.; Liu, D.; Santos, H. A.
46
47 Electrospun Fibrous Architectures for Drug Delivery, Tissue Engineering and Cancer
48
49 Therapy. *Advanced Functional Materials.* 2019.
50
51 <https://doi.org/10.1002/adfm.201802852>.
- 52
53
54 (150) Lancina, M. G.; Singh, S.; Kompella, U. B.; Husain, S.; Yang, H. Fast Dissolving
55
56 Dendrimer Nanofiber Mats as Alternative to Eye Drops for More Efficient
57
58
59
60

- 1
2
3 Antiglaucoma Drug Delivery. *ACS Biomater. Sci. Eng.* **2017**, 3 (8), 1861–1868.
4
5 <https://doi.org/10.1021/acsbmaterials.7b00319>.
6
7
8 (151) Xia, G.; Zhang, H.; Cheng, R.; Wang, H.; Song, Z.; Deng, L.; Huang, X.; Santos, H.
9
10 A.; Cui, W. Localized Controlled Delivery of Gemcitabine via Microsol Electrospun
11
12 Fibers to Prevent Pancreatic Cancer Recurrence. *Adv. Healthc. Mater.* **2018**, 7 (18), 1–
13
14 13. <https://doi.org/10.1002/adhm.201800593>.
15
16
17 (152) Indermun, S.; Govender, M.; Kumar, P.; Choonara, Y. E.; Pillay, V. *Stimuli-*
18
19 *Responsive Polymers as Smart Drug Delivery Systems: Classifications Based on*
20
21 *Carrier Type and Triggered-Release Mechanism*; Elsevier Ltd., 2018.
22
23 <https://doi.org/10.1016/b978-0-08-101997-9.00002-3>.
24
25
26 (153) Wang, J.; Wang, G.; Shan, H.; Wang, X.; Wang, C.; Zhuang, X.; Ding, J.; Chen, X.
27
28 Gradiently Degraded Electrospun Polyester Scaffolds with Cytostatic for Urothelial
29
30 Carcinoma Therapy. *Biomater. Sci.* **2019**, 7 (3), 963–974.
31
32 <https://doi.org/10.1039/c8bm01317a>.
33
34
35 (154) Xie, X.; Zheng, X.; Han, Z.; Chen, Y.; Zheng, Z.; Zheng, B.; He, X.; Wang, Y.;
36
37 Kaplan, D. L.; Li, Y.; et al. A Biodegradable Stent with Surface Functionalization of
38
39 Combined-Therapy Drugs for Colorectal Cancer. *Adv. Healthc. Mater.* **2018**, 7 (24).
40
41 <https://doi.org/10.1002/adhm.201801213>.
42
43
44 (155) Bonadies, I.; Maglione, L.; Ambrogi, V.; Paccez, J. D.; Zerbini, L. F.; Rocha e Silva,
45
46 L. F.; Picanço, N. S.; Tadei, W. P.; Grafova, I.; Grafov, A.; et al. Electrospun
47
48 Core/Shell Nanofibers as Designed Devices for Efficient Artemisinin Delivery. *Eur.*
49
50 *Polym. J.* **2017**, 89 (January), 211–220.
51
52 <https://doi.org/10.1016/j.eurpolymj.2017.02.015>.
53
54
55 (156) Ramachandran, R.; Junnuthula, V. R.; Gowd, G. S.; Ashokan, A.; Thomas, J.;
56
57
58
59
60

- 1
2
3 Peethambaran, R.; Thomas, A.; Unni, A. K. K.; Panikar, D.; Nair, S. V.; et al.
4
5
6 Theranostic 3-Dimensional Nano Brain-Implant for Prolonged and Localized
7
8 Treatment of Recurrent Glioma. *Sci. Rep.* **2017**, *7*. <https://doi.org/10.1038/srep43271>.
9
- 10
11 (157) Shin, H. M.; Ju, Y.; Kim, G.; Lee, J. W.; Seo, M. W.; Sim, J. H.; Yang, J.; Noh, S.;
12
13 Kim, J.; Kim, H. R. Recyclable Cytokines on Short and Injectable Polylactic Acid
14
15 Fibers for Enhancing T-Cell Function. *Adv. Funct. Mater.* **2019**, *29* (14).
16
17 <https://doi.org/10.1002/adfm.201808361>.
18
19
- 20
21 (158) Baishya, H. Application of Mathematical Models in Drug Release Kinetics of
22
23 Carbidopa and Levodopa ER Tablets. *J. Dev. Drugs* **2017**, *06* (02), 1–8.
24
25 <https://doi.org/10.4172/2329-6631.1000171>.
26
27
- 28
29 (159) Tiwari, S. K.; Tzezana, R.; Zussman, E.; Venkatraman, S. S. Optimizing Partition-
30
31 Controlled Drug Release from Electrospun Core-Shell Fibers. *Int. J. Pharm.* **2010**, *392*
32
33 (1–2), 209–217. <https://doi.org/10.1016/j.ijpharm.2010.03.021>.
34
35
- 36
37 (160) He, M.; Xue, J.; Geng, H.; Gu, H.; Chen, D.; Shi, R.; Zhang, L. Fibrous Guided Tissue
38
39 Regeneration Membrane Loaded with Anti-Inflammatory Agent Prepared by Coaxial
40
41 Electrospinning for the Purpose of Controlled Release. *Appl. Surf. Sci.* **2015**, *335*, 121–
42
43 129. <https://doi.org/10.1016/j.apsusc.2015.02.037>.
44
45
- 46
47 (161) Yang, J. M.; Zha, L. sheng; Yu, D. G.; Liu, J. Coaxial Electrospinning with Acetic
48
49 Acid for Preparing Ferulic Acid/Zein Composite Fibers with Improved Drug Release
50
51 Profiles. *Colloids Surfaces B Biointerfaces* **2013**, *102*, 737–743.
52
53 <https://doi.org/10.1016/j.colsurfb.2012.09.039>.
54
55
- 56
57 (162) Carson, D.; Jiang, Y.; Woodrow, K. A. Tunable Release of Multiclass Anti-HIV Drugs
58
59 That Are Water-Soluble and Loaded at High Drug Content in Polyester Blended
60
Electrospun Fibers. *Pharm. Res.* **2016**, *33* (1), 125–136.

- 1
2
3 <https://doi.org/10.1007/s11095-015-1769-0>.
- 4
5
6 (163) Yu, H.; Jia, Y.; Yao, C.; Lu, Y. PCL/PEG Core/Sheath Fibers with Controlled Drug
7
8 Release Rate Fabricated on the Basis of a Novel Combined Technique. *Int. J. Pharm.*
9
10 **2014**, *469* (1), 17–22. <https://doi.org/10.1016/j.ijpharm.2014.04.045>.
- 11
12
13 (164) Eskitoros-Togay, M.; Bulbul, Y. E.; Dilsiz, N. Quercetin-Loaded and Unloaded
14
15 Electrospun Membranes: Synthesis, Characterization and in Vitro Release Study. *J.*
16
17 *Drug Deliv. Sci. Technol.* **2018**, *47* (March), 22–30.
18
19 <https://doi.org/10.1016/j.jddst.2018.06.017>.
- 20
21
22 (165) Fu, Y.; Li, X.; Ren, Z.; Mao, C.; Han, G. Multifunctional Electrospun Nanofibers for
23
24 Enhancing Localized Cancer Treatment. *Small* **2018**, *1801183*, 1801183.
25
26 <https://doi.org/10.1002/sml.201801183>.
- 27
28
29 (166) Wilhelm, S.; Tavares, A. J. .; Dai, Q.; Ohta, S.; Audet, J.; Dvorak, H. F. .; Chan, W. C.
30
31 W. . Analysis of Nanoparticle Delivery to Tumours. *Nat. Rev. Mater.* **2016**, *1* (5),
32
33 16014. <https://doi.org/10.1038/natrevmats.2016.14>.
- 34
35
36 (167) Wang, Z.; Ma, R.; Yan, L.; Chen, X.; Zhu, G. Combined Chemotherapy and
37
38 Photodynamic Therapy Using a Nanohybrid Based on Layered Double Hydroxides to
39
40 Conquer Cisplatin Resistance. *Chem. Commun.* **2015**, *51* (58), 11587–11590.
41
42 <https://doi.org/10.1039/c5cc04376j>.
- 43
44
45 (168) Liu, Y.; Zhang, X.; Zhou, M.; Nan, X.; Chen, X.; Zhang, X. Mitochondrial-Targeting
46
47 Lonidamine-Doxorubicin Nanoparticles for Synergistic Chemotherapy to Conquer
48
49 Drug Resistance. *ACS Appl. Mater. Interfaces* **2017**, *9* (50), 43498–43507.
50
51 <https://doi.org/10.1021/acsami.7b14577>.
- 52
53
54 (169) Blanco, E.; Shen, H.; Ferrari, M. Principles of Nanoparticle Design for Overcoming
55
56 Biological Barriers to Drug Delivery. *Nat. Biotechnol.* **2015**, *33* (9), 941–951.
57
58
59
60

- 1
2
3 <https://doi.org/10.1038/nbt.3330>.
4
5
6 (170) Yang, G.; Wang, J.; Wang, Y.; Li, L.; Guo, X.; Zhou, S. An Implantable Active-
7 Targeting Micelle-in-Nanofiber Device for Efficient and Safe Cancer Therapy. *ACS*
8 *Nano* **2015**, *9* (2), 1161–1174. <https://doi.org/10.1021/nn504573u>.
9
10
11
12
13 (171) He, Y.; Li, X.; Ma, J.; Ni, G.; Yang, G.; Zhou, S. Programmable Codelivery of
14 Doxorubicin and Apatinib Using an Implantable Hierarchical-Structured Fiber Device
15 for Overcoming Cancer Multidrug Resistance. *Small* **2019**, *15* (8).
16
17
18
19
20 <https://doi.org/10.1002/sml.201804397>.
21
22
23 (172) Puri, A.; Loomis, K.; Smith, B.; Lee, J.-H.; Yavlovich, A.; Heldman, E.; Blumenthal,
24 R. Lipid-Based Nanoparticles as Pharmaceutical Drug Carriers: From Concepts to
25 Clinic. *Crit Rev Ther Drug Carr. Syst* **2009**, *26* (6), 523–580.
26
27
28
29
30 (173) Shevtsov, M. A.; Yakovleva, L. Y.; Nikolaev, B. P.; Marchenko, Y. Y.; Dobrodumov,
31 A. V.; Onokhin, K. V.; Onokhina, Y. S.; Selkov, S. A.; Mikhrina, A. L.; Guzhova, I.
32 V.; et al. Tumor Targeting Using Magnetic Nanoparticle Hsp70 Conjugate in a Model
33 of C6 Glioma. *Neuro. Oncol.* **2014**, *16* (1), 38–49.
34
35
36
37
38
39 <https://doi.org/10.1093/neuonc/not141>.
40
41
42 (174) Allen, T. M.; Cullis, P. R. Liposomal Drug Delivery Systems: From Concept to
43 Clinical Applications. *Adv. Drug Deliv. Rev.* **2013**, *65* (1), 36–48.
44
45
46
47 <https://doi.org/10.1016/j.addr.2012.09.037>.
48
49 (175) Kirpotin, D. B.; Drummond, D. C.; Shao, Y.; Shalaby, M. R.; Hong, K.; Nielsen, U.
50 B.; Marks, J. D.; Benz, C. C.; Park, J. W. Antibody Targeting of Long-Circulating
51 Lipidic Nanoparticles Does Not Increase Tumor Localization but Does Increase
52 Internalization in Animal Models. *Cancer Res.* **2006**, *66* (13), 6732–6740.
53
54
55
56
57
58 <https://doi.org/10.1158/0008-5472.CAN-05-4199>.
59
60

- 1
2
3 (176) Ventola, C. L. Progress in Nanomedicine: Approved and Investigational Nanodrugs. *P*
4
5 *T* **2017**, *42* (12), 742–755. <https://doi.org/10.1016/j.psychres.2007.07.030>.
6
7
- 8 (177) Narang, A.; Chang, R.-K.; Hussain, M. A. Pharmaceutical Development and
9
10 Regulatory Considerations for Nanoparticles and Nanoparticulate Drug Delivery
11
12 Systems. *J. Pharm. Sci.* **2013**, *102* (11), 3867–3882. <https://doi.org/10.1002/jps.23691>.
13
14
- 15 (178) Sohrabi, A.; Shaibani, P. M.; Etayash, H.; Kaur, K.; Thundat, T. Sustained Drug
16
17 Release and Antibacterial Activity of Ampicillin Incorporated Poly(Methyl
18
19 Methacrylate)-Nylon6 Core/Shell Nanofibers. *Polym. (United Kingdom)* **2013**, *54* (11),
20
21 2699–2705. <https://doi.org/10.1016/j.polymer.2013.03.046>.
22
23
24
- 25 (179) Qian, W.; Yu, D. G.; Li, Y.; Liao, Y. Z.; Wang, X.; Wang, L. Dual Drug Release
26
27 Electrospun Core-Shell Nanofibers with Tunable Dose in the Second Phase. *Int. J.*
28
29 *Mol. Sci.* **2014**, *15* (1), 774–786. <https://doi.org/10.3390/ijms15010774>.
30
31
- 32 (180) Chen, Y.; Liu, S.; Hou, Z.; Ma, P.; Yang, D.; Li, C.; Lin, J. Multifunctional
33
34 Electrospinning Composite Fibers for Orthotopic Cancer Treatment in Vivo. *Nano*
35
36 *Res.* **2015**, *8* (6), 1917–1931. <https://doi.org/10.1007/s12274-014-0701-y>.
37
38
- 39 (181) Samadi, S.; Moradkhani, M.; Beheshti, H.; Irani, M.; Aliabadi, M. Fabrication of
40
41 Chitosan/Poly(Lactic Acid)/Graphene Oxide/TiO₂ composite Nanofibrous Scaffolds
42
43 for Sustained Delivery of Doxorubicin and Treatment of Lung Cancer. *Int. J. Biol.*
44
45 *Macromol.* **2018**, *110*, 416–424. <https://doi.org/10.1016/j.ijbiomac.2017.08.048>.
46
47
48
- 49 (182) Han, D.; Sasaki, M.; Yoshino, H.; Kofuji, S.; Sasaki, A. T.; Steckl, A. J. In-Vitro
50
51 Evaluation of MPA-Loaded Electrospun Coaxial Fiber Membranes for Local
52
53 Treatment of Glioblastoma Tumor Cells. *J. Drug Deliv. Sci. Technol.* **2017**, *40*, 45–50.
54
55 <https://doi.org/10.1016/j.jddst.2017.05.017>.
56
57
- 58 (183) Irani, M.; Mir Mohamad Sadeghi, G.; Haririan, I. A Novel Biocompatible Drug
59
60

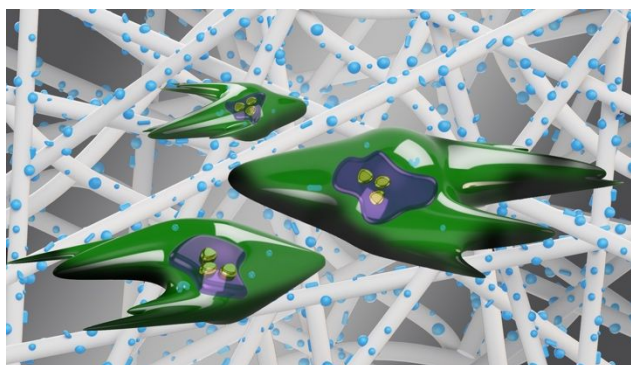
1
2
3 Delivery System of Chitosan/Temozolomide Nanoparticles Loaded PCL-PU
4
5 Nanofibers for Sustained Delivery of Temozolomide. *Int. J. Biol. Macromol.* **2017**, *97*,
6
7 744–751. <https://doi.org/10.1016/j.ijbiomac.2017.01.073>.
8
9
10
11
12
13

14 **Electrospun Nanofibers for Drug Delivery and Biosensing**

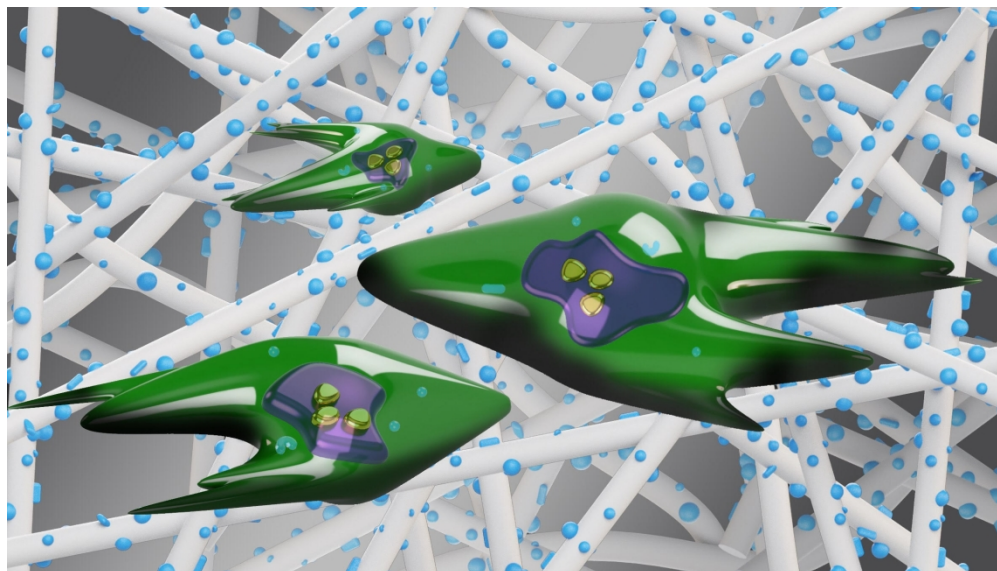
15
16
17
18 Conor Cleeton¹, Antonios Keirouz¹, Xianfeng Chen², Norbert Radacsi^{1*}
19
20
21

22 ¹The School of Engineering, Institute for Materials and Processes, The University of
23 Edinburgh, Robert Stevenson Road, Edinburgh, EH9 3FB, United Kingdom
24

25
26 ²School of Engineering, Institute for Bioengineering, The University of Edinburgh, King's
27 Buildings, Mayfield Road, Edinburgh EH9 3JL, United Kingdom
28
29
30
31



44 This review describes the fabrication, properties, and applications of electrospun nanofibers
45 as promising materials for the construction of nanoscale biosensors and therapeutic platforms
46 for cancer diagnosis and treatment.
47
48
49
50
51
52
53
54
55
56
57
58
59
60



This review describes the fabrication, properties, and applications of electrospun nanofibers as promising materials for the construction of nanoscale biosensors and therapeutic platforms for cancer diagnosis and treatment.